

Oxidative coupling of methane over lithium promoted magnesia

Citation for published version (APA):

Kasteren, van, J. M. N. (1990). *Oxidative coupling of methane over lithium promoted magnesia*. [Phd Thesis 1 (Research TU/e / Graduation TU/e), Chemical Engineering and Chemistry]. Technische Universiteit Eindhoven. <https://doi.org/10.6100/IR339832>

DOI:

[10.6100/IR339832](https://doi.org/10.6100/IR339832)

Document status and date:

Published: 01/01/1990

Document Version:

Publisher's PDF, also known as Version of Record (includes final page, issue and volume numbers)

Please check the document version of this publication:

- A submitted manuscript is the version of the article upon submission and before peer-review. There can be important differences between the submitted version and the official published version of record. People interested in the research are advised to contact the author for the final version of the publication, or visit the DOI to the publisher's website.
- The final author version and the galley proof are versions of the publication after peer review.
- The final published version features the final layout of the paper including the volume, issue and page numbers.

[Link to publication](#)

General rights

Copyright and moral rights for the publications made accessible in the public portal are retained by the authors and/or other copyright owners and it is a condition of accessing publications that users recognise and abide by the legal requirements associated with these rights.

- Users may download and print one copy of any publication from the public portal for the purpose of private study or research.
- You may not further distribute the material or use it for any profit-making activity or commercial gain
- You may freely distribute the URL identifying the publication in the public portal.

If the publication is distributed under the terms of Article 25fa of the Dutch Copyright Act, indicated by the "Taverne" license above, please follow below link for the End User Agreement:

www.tue.nl/taverne

Take down policy

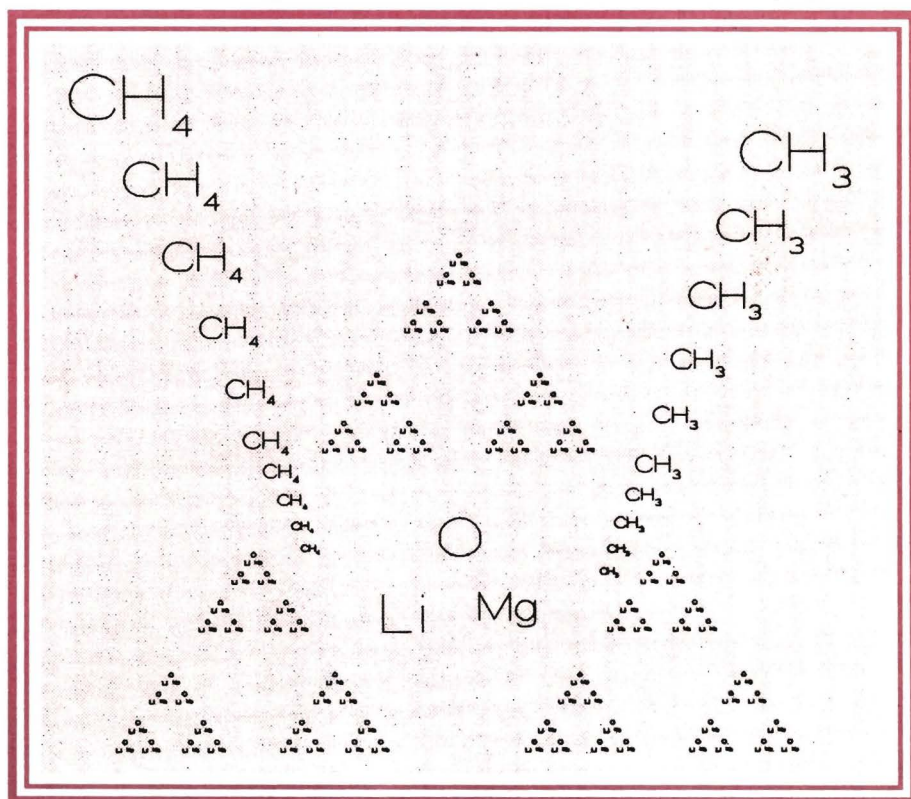
If you believe that this document breaches copyright please contact us at:

openaccess@tue.nl

providing details and we will investigate your claim.

OXIDATIVE COUPLING OF METHANE OVER LITHIUM PROMOTED MAGNESIA

J.M.N. VAN KASTEREN



**OXIDATIVE COUPLING
OF METHANE OVER
LITHIUM PROMOTED MAGNESIA**

Proefschrift

ter verkrijging van de graad van doctor aan
de Technische Universiteit Eindhoven, op gezag
van de Rector Magnificus, prof. ir. M. Tels, voor
een commissie aangewezen door het College
van Dekanen in het openbaar te verdedigen
op vrijdag 2 november 1990 te 16.00 uur

door

Johannes Maria Nicolaas van Kasteren
geboren te Heerlen

Dit proefschrift is goedgekeurd door de promotoren:

**Prof. dr. ir. K. van der Wiele
Prof. dr. ir. G.B.M.M. Marin**

copromotor:

Dr. ir. J.H.B.J. Hoebink

Aan mijn Ouders
Aan Riet

Wie zal zeggen wat hij wil, zal horen wat hij niet wil.

Terentius Andr. 920

SAMENVATTING

Het besef van de eindigheid van de aardolievoorraden en het toegenomen aantal vindplaatsen van aardgas hebben geleid tot een sterke belangstelling voor het gebruik van aardgas als grondstof voor de chemische industrie. De meeste locaties van de grote aardgasvelden zijn van dien aard dat transport over zeer grote afstanden nodig is. Dit transport van aardgas is gecompliceerd en duur en maakt het zoeken naar methoden om aardgas bij de bron om te zetten in makkelijker te transporteren chemicaliën interessant. Aangezien aardgas hoofdzakelijk uit methaan bestaat, kan de chemische omzetting van aardgas zich voornamelijk beperken tot het bestuderen van de chemische omzetting van methaan.

Omzetting van aardgas tot bruikbare componenten (zoals methanol of benzine) geschiedt momenteel vrijwel uitsluitend via de zogenaamde indirecte route die de productie van synthese gas (CO/H_2) door middel van steam reforming bevat. Dit synthese gas is om te zetten in methanol, etheen of benzine. Echter, directe conversie van methaan tot deze nuttige koolwaterstoffen, waarbij de omslachtige en energetisch ongunstige steam reformingsstap vermeden wordt, vormt een veel aantrekkelijker alternatief.

Dit proefschrift betreft een studie naar de directe omzetting van methaan tot etheen via de zogenaamde oxydatieve koppeling: methaan wordt met behulp van zuurstof in aanwezigheid van een katalysator direct geconverteerd naar etheen en water. Centraal in dit onderzoek staat de lithium gedoteerde magnesiumoxyde (Li/MgO) katalysator. Naast aandacht voor de bereidingswijze is de werking en invloed van de katalysator op de methaanomzetting uitvoerig onderzocht.

De bereidingswijze van de Li/MgO - katalysator blijkt vooral een sterke invloed uit te oefenen op het initiële activiteitsverloop van het koppelingsproces. Dit effect is toe te schrijven aan het lithiumgehalte, het specifieke oppervlak (m^2/g) en de poriënstructuur. Lithium is duidelijk verantwoordelijk voor de hoge C_{2+} opbrengst. Reeds zeer kleine hoeveelheden lithium (0.2wt%) toegevoegd aan het MgO blijken voldoende te zijn voor een hoge C_{2+} yield. Speciaal de aanwezigheid van de lithiumcarbonaاتفase blijkt hierbij een sleutelrol te vervullen.

Desaktivering van de Li/MgO katalysator treedt op door verlies van lithium. Dit verlies wordt hoofdzakelijk veroorzaakt door reactie van de aanwezige lithiumfasen met water waarbij lithiumhydroxyde gevormd wordt. Dit lithiumhydroxyde is zeer vluchtig onder reactie omstandigheden (800°C) en dampst zodoende uit de katalysator om "downstream" weer neer te slaan. Daarnaast treedt lithiumverlies op door reactie van het lithium met

de quartz reactorwand. De ontstane lithiümsilikaten verhinderen het lithium verder deel te nemen aan het katalytische proces.

Het mechanisme van de werking van de Li/MgO katalysator is bestudeerd met behulp van de steady-state isotopic transiënt kinetic analysis (SSITKA) techniek met $^{13}\text{CH}_4$ and $^{18}\text{O}_2$ als isotoop. Deze metingen zijn uitgevoerd in een speciaal daarvoor ontworpen proefopstelling. Deze experimenten tonen aan dat bij 800°C de zuurstofadsorptie een belangrijke rol speelt en dat de methaanadsorptie verwaarloosbaar is. Tevens blijkt er ook geen noemenswaardige hoeveelheid ^{13}C te worden in gebouwd in de katalysator. Dit toont aan dat de lithiumcarbonaantleding geen deel uitmaakt van de katalytische cyclus. De actieve zuurstofspecies wordt waarschijnlijk gevormd via een oxydische lithiumfase. Het verlies van de actieve (lithium)fase wordt aangevuld vanuit de lithiumcarbonaafase door lithiumcarbonaantleding. Het mechanisme van de methaan aktivering kan beschreven worden met een ELEY - RIDEAL mechanisme waarbij methaan vanuit de gasfase reageert met een actieve zuurstofspecies op het oppervlak van de katalysator.

Het mechanisme van ethaan- en etheenvorming vanuit methaan is uitvoerig bestudeerd in een lage druk reactor (100 Pa). Het proces blijkt te bestaan uit een gecompliceerd reactienetwerk van homogene radicaal reacties en heterogene aktiveringsreacties. Ethaan wordt primair gevormd uit de koppeling van twee methylradicalen in de gasfase. Deze methylradicalen worden gevormd door waterstofabstractie van methaan aan het katalysatoroppervlak. Zowel aan het katalysatoroppervlak als in de gasfase reageert ethaan tot etheen en etheen tot koolmonoxyde (CO). Koolmonoxyde wordt voornamelijk aan het katalysatoroppervlak geoxydeerd tot CO_2 . De gasfasereacties zijn essentieel, omdat de methylradicalen aan het katalysatoroppervlak hoofdzakelijk oxyderen tot CO .

Met behulp van een gelijkspanningsontlading in argon is de invloed van de Li/MgO katalysator op radicaalrecombineringsreacties onderzocht. In de positieve zuil van het argon plasma wordt de functie van de katalysator als versneller van de methaandissociatie overgenomen door argon metastabielen. Met deze techniek is het mogelijk CH_3 en CH_2 radicalen direct vanuit methaan te produceren. De Li/MgO katalysator blijkt radicaalrecombineringsreacties nauwelijks te beïnvloeden. De rol van de Li/MgO katalysator in het methaankoppelingsproces kan samengevat worden als een methaanaktuator die grote hoeveelheden methylradicalen in de gasfase veroorzaakt. Dit levert automatisch een verhoogde ethaanvorming op.

Met behulp van bijmengexperimenten bij lage druk (100 Pa) is het verschil tussen de aktivering van methaan, ethaan en etheen door Li/MgO bepaald. Het blijkt dat ethaan een faktor 1,5 makkelijker te oxyderen is dan etheen en etheen weer een faktor 2,6 makkelijker dan methaan. Met behulp van computersimulaties van het volgreactie -

model en deze onderlinge reactiviteiten blijkt een (theoretische) C_{2+} opbrengst van ongeveer 35% mogelijk te zijn. In de praktijk zijn echter de homogene gasfase reacties de oorzaak van een veel lagere C_{2+} opbrengst. Modelleren van het selectiviteitsverloop van een sterk verouderde katalysator, dat sterk lijkt op het selectiviteitspatroon van de homogene gasfase oxydatieve methaankoppeling, resulteerde in een activiteitsverschil tussen ethaan en methaan van 57 en tussen etheen en methaan van 19. De maximale C_{2+} opbrengst die met deze getallen te behalen is bedraagt 6%. Met een verse Li/MgO katalysator blijkt in de praktijk een C_{2+} opbrengst mogelijk van 16 - 18% onder identieke omstandigheden. Verdergaande optimalisatie van de wisselwerking tussen de homogene en heterogene reacties moet een C_{2+} opbrengst van 25% bij een C_{2+} selectiviteit van 60% mogelijk maken. Deze laatste getallen zijn waarden waarbij de directe omzetting van methaan tot etheen commercieel aantrekkelijk wordt ten opzichte van de huidige etheen productie uit aardolie.

Concluderend is met dit onderzoek een goed inzicht verkregen in de werking van de Li/MgO katalysator voor de directe conversie van methaan tot etheen. De Li/MgO katalysator blijkt perspectief te bieden voor verder onderzoek, waarbij de nadruk vooral zal moeten liggen op verbetering van de stabiliteit.

SUMMARY

The awareness of the limited reserves of oil and the increased number of finding spots of natural gas have led to an increased interest for the use of natural gas as feedstock for the chemical industry. The locations of the large natural gas fields are often found in remote areas necessitating the need for transport of natural gas over long distances. This transport of natural gas is complicated and expensive and is one of the reasons that methods to convert natural gas into more easily transportable chemicals at the well are enjoying great attention. As natural gas primarily contains methane, the conversion of natural gas can be restricted to the study of the conversion of methane into useful chemicals.

Nowadays the conversion of natural gas into components like methanol or gasoline is almost exclusively carried out via the so-called indirect route which comprises the production of synthesis gas (CO/H_2) via steam reforming. Synthesis gas in turn can be converted readily into useful hydrocarbons like methanol, ethylene or gasoline. However, the direct conversion of methane into useful hydrocarbons, avoiding the cumbersome and energetically unfavoured steam reforming process, forms a much more attractive alternative.

This thesis is concerned with the study of the direct conversion of methane into ethylene via the so-called oxidative coupling process: methane is converted into ethylene and water with the aid of oxygen in the presence of a catalyst. This study is focussed on the lithium doped magnesia (Li/MgO) catalyst. Beside attention for the preparation method of this catalyst, the working principle and the influence of this catalyst on the methane conversion have been studied extensively.

The synthesis method of the Li/MgO catalyst especially influences the initial activity of the catalyst. This effect is due to the lithium content, specific surface area (m^2/g) and pore structure. Lithium is clearly responsible for the high C_{2+} yield observed with this catalyst. Already very small amounts of lithium added to MgO are sufficient for a high C_{2+} yield. The presence of the lithium carbonate phase appears to fulfil a keyrole in this.

Deactivation of the Li/MgO catalyst is caused by loss of lithium. This loss is mainly caused by reaction of the lithium phases present in the catalyst with the water vapour resulting in lithium hydroxide (LiOH). This LiOH is volatile under the applied reaction temperatures of 800°C leading to evaporation and transport of the lithium with the gas stream out of the reactor. Beside this evaporation effect a part of the lithium gets lost via reaction with the quartz reactor wall. The lithium silicates thus formed prevent

further participation of the lithium in the catalytic process.

The working principle of the Li/MgO catalyst has been elucidated with the so-called steady-state isotopic transient kinetic analysis technique (SSITKA) using $^{13}\text{CH}_4$ and $^{18}\text{O}_2$ as isotopes. These experiments were carried out in a specially designed set-up. From these experiments it is concluded that at 800°C only oxygen adsorption was significant and that methane adsorption was negligible. Hardly any ^{13}C is built into the catalyst indicating that there exists no large pool of a carbon containing species at the catalyst surface, which is taking part in the catalytic cycle. The active oxygen species is created via an oxidic lithium phase. The lithium carbonate phase present acts as a source of lithium by replenishing the active lithium phase, which is lost by evaporation of the hydroxide. The mechanism of the methane activation can be described by an ELEY - RIDEAL mechanism in which methane reacts from the gas phase with an adsorbed active oxygen species to a methyl radical, which is released into the gas phase.

The mechanism of ethane and ethylene formation has been elucidated by experiments at reduced pressures (100 Pa). The mechanism consists of a complicated network of homogeneous gas phase and heterogeneous surface reactions. Ethane is primarily formed via the coupling of two methyl radicals in the gas phase. The methyl radicals are formed by hydrogen abstraction from methane at the catalyst surface. The dehydrogenation of ethane into ethylene and the oxidation of ethylene into carbon monoxide are taking place both in the gas phase and on the catalyst surface. The reaction of CO into CO_2 is predominantly a catalytic reaction. The gas phase reactions are essential, because at the catalyst surface mainly total oxidation of the methyl radicals into CO takes place.

The influence of the Li/MgO catalyst on radical recombination reactions has been studied with the aid of a d.c. electrical discharge in argon. In the positive column of the argon plasma, argon metastables take over the methane dissociation function of the catalyst. In this way CH_3 and CH_2 radicals are created directly from methane. The Li/MgO catalyst does not appear to influence the radical coupling reactions strongly. The role of the Li/MgO catalyst can be summarized as a methane activator releasing large amounts of methyl radicals into the gas phase. This stimulates the formation of ethane.

The difference in activity of ethane, ethylene and methane for hydrogen abstraction by Li/MgO has been studied by admixing experiments at reduced pressures (100 Pa). It appears that ethane is activated a factor 1.5 faster than ethylene and that ethylene in turn is activated a factor 2.6 faster than methane. Based on these measured activity differences and a computer simulation of the consecutive reaction model it is shown that a C_{2+} yield of 35% is (theoretically) possible. In reality however, homogeneous gas phase reactions are the cause of much lower C_{2+} yields. Modelling of the selectivity

pattern of an aged catalyst, which selectivity pattern strongly resembles that of the homogeneous gas phase methane coupling process, resulted in a reactivity difference between ethane and methane of 57 and between ethylene and methane of 19. These numbers reduce the maximum attainable C_{2+} yield to 6%. With a fresh Li/MgO catalyst C_{2+} yields of 16 - 18% have been achieved under the same conditions. Further optimization of the interaction between homogeneous gas phase and heterogenous surface reactions should make C_{2+} yields of 25% at 60% C_{2+} selectivity attainable. These numbers are the values at which the methane coupling process becomes commercially attractive compared to the present ethylene production method via naphtha cracking.

Summarizing this study has provided a good insight in the working principle of the Li/MgO catalyst for the direct conversion of methane into ethylene. It is shown that the Li/MgO offers perspectives for future use provided that improvement of the stability of the catalyst is achieved.

CONTENTS

| | | |
|------------------|---|----------|
| | SAMENVATTING-SUMMARY | 5 |
| Chapter 1 | INTRODUCTION | |
| | 1.1 Conversion of natural gas into useful chemicals | 15 |
| | 1.2 Thermodynamics | 17 |
| | 1.3 Literature summary | 18 |
| | 1.4 Aims and outline of this thesis | 23 |
| Chapter 2 | Li/MgO CATALYST PREPARATION AND PERFORMANCE | |
| | 2.1 Introduction | 27 |
| | 2.2 Catalyst preparation and continuous oxidation equipment | 27 |
| | 2.3 The influence of catalyst preparation on the coupling performance | 29 |
| | 2.4 The influence of catalyst pretreatment on the coupling performance | 31 |
| | 2.5 Conclusions | 32 |
| Chapter 3 | CATALYST DYNAMICS AND DEACTIVATION MECHANISM | |
| | 3.1 Introduction | 35 |
| | 3.2 Experimental | 35 |
| | 3.3 Catalyst stability | 37 |
| | 3.4 Catalyst deactivation | 39 |
| | 3.5 Working principle of the Li/MgO catalyst | 40 |
| | 3.6 Elucidation of the Li/MgO catalyst working principle by steady-state isotopic transient kinetic analysis | 42 |
| | 3.7 Conclusions | 46 |

| | | |
|-----------|--|----|
| Chapter 4 | ANALYSIS OF THE REACTION NETWORK | |
| | 4.1 Introduction | 49 |
| | 4.2 Experimental | 50 |
| | 4.3 The role of the catalyst in the methane coupling process | 53 |
| | 4.4 The role of the catalyst in consecutive reactions | 57 |
| | 4.5 Interaction of radicals with Li/MgO | 61 |
| | 4.6 Conclusions | 66 |
| Chapter 5 | KINETIC MODELLING | |
| | 5.1 Introduction | 69 |
| | 5.2 Experimental | 70 |
| | 5.3 Mass transfer limitations | 70 |
| | 5.4 Kinetic modelling | 72 |
| | 5.5 Conclusions | 77 |
| Chapter 6 | FINAL DISCUSSION | 79 |
| | LIST OF PUBLICATIONS | 83 |
| | DANKWOORD | 85 |
| | CURRICULUM VITAE | 87 |

CHAPTER 1

INTRODUCTION

1.1 CONVERSION OF NATURAL GAS INTO USEFUL CHEMICALS

The prospective shortage of oil as carbon feedstock for the chemical industry has started renewed attention for the use of natural gas. On a global basis, both oil and natural gas have limited reserves, but on current usage patterns a shortage of oil will occur first¹ (Table 1.1.1).

Table 1.1.1. Proven world reserves and consumption for oil and gas in 1988¹.

| 1988 | Oil (10 ⁹ tons) | Natural Gas (10 ⁹ ton oil equivalent) |
|---------------------------|-------------------------------|---|
| Reserves ² (R) | 134.5 | 100.6 |
| Production (P) | 3 | 1.7 |
| R/P (years) | 45 | 57 |
|) Estimated | | |

In addition to this shortage perspective of oil, natural gas is found quite often in remote areas. As it is very difficult and expensive to transport natural gas it is desirable to convert it into easier transportable forms like methanol or higher hydrocarbons. Natural gas is primarily methane. Thermodynamically methane is the most stable hydrocarbon, which means that its conversion into higher hydrocarbons requires a considerable effort. Figure 1.1.1 shows the main strategies for methane conversion. The routes can be divided into two groups: direct conversion and indirect conversion into hydrocarbons. The indirect conversion of methane is performed via steam reforming of methane into synthesis gas (CO/H₂). This can be converted into hydrocarbons either directly via the Fischer - Tropsch process or indirectly via methanol. A plant for the conversion of natural gas into middle distillates via a Fischer - Tropsch like process is projected in Malaysia by Shell (SMDS process).² The conversion of natural gas via synthesis gas and methanol has been commercialized in New Zealand: The Methane-To-Gasoline (MTG) process. It is economically attractive due to the local circumstances: a remote area and the total lack of oil.

The direct methane conversion into hydrocarbons can be carried out in various ways. Practical applications have been found in the acetylene production via either the electric arc or the thermal cracking process. The disadvantage of both processes is the large

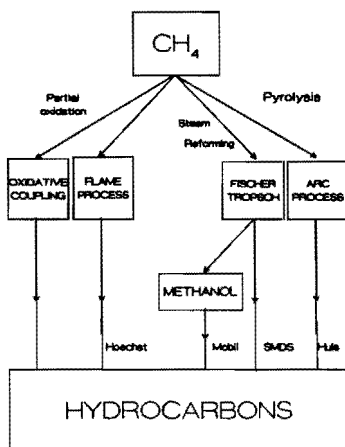
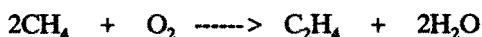


Figure 1.1.1. Possible routes for methane conversion to hydrocarbons.

generation of carbon as by-product and the low yield to acetylene (< 30%). Moreover, the electric arc process is only attractive if cheap electricity is available. The acetylene production from methane has also been carried out by partial oxidation at 1500°C. Again the C_{2+} yield never exceeded 30%, the remainder being CO, CO₂ and H₂. The disadvantage of this process is the extremely high temperature at which it has to be carried out and the formation of soot which cannot be avoided. A very effective heat recovery is economically essential for these processes.

A more attractive route for the direct conversion of methane into C_{2+} hydrocarbons is the oxidative coupling of methane. Methane is directly converted into ethylene in the presence of oxygen:



This reaction is thermodynamically feasible at all useful temperatures. Problems are associated with the formation of thermodynamically more favoured total oxidation products (CO, CO₂). Challenging is to minimize these total oxidation reactions by kinetically controlling the reaction, i.e. by applying a suitable catalyst.

Economic evaluation studies of this process³ revealed that C_{2+} yields of 25% with a minimum C_{2+} selectivity of 65% are needed to have a commercial process which can compete with the established technology of naphtha cracking into ethylene.

The catalytic oxidative coupling process should preferably be carried out in a fluidized bed reactor, because of the good heat exchange that is needed to control the highly exothermic oxidation reactions. The best catalysts developed so far produce C_{2+} yields of about 20%. Despite the fact that these results are promising, still the development

of catalysts with higher C_{2+} yields is needed.

1.2 THERMODYNAMICS

Before the direct conversion of methane with oxygen into useful hydrocarbons can be considered the thermodynamics of the methane pyrolysis should be examined. Figure 1.2.1 shows the Gibbs free energy of formation of possible pyrolysis products from methane as function of the temperature.

It is clear from Figure 1.2.1 that very high temperatures are needed to favour the higher hydrocarbon production from methane. Since carbon formation is possible at considerably lower temperatures, it is challenging to optimize the hydrocarbon formation via kinetics. Recently Chevron workers⁴ claim an inhibiting effect of catalytic material on the coke formation during methane pyrolysis. Van der Zwet et al.⁵ reported that the coke formation does not depend on the kind of catalytic material, but on the surface area. They concluded that the lowest surface area to reactor volume produced the lowest amount of coke, i.e. the empty tube reactor! In practice methane pyrolysis is not a very attractive process due to the formation of large amounts of coke, which are very difficult to prevent.

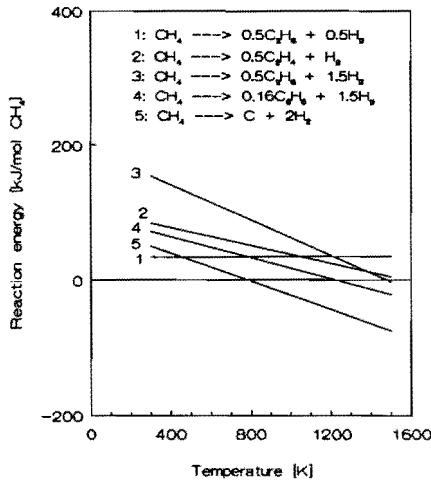


Figure 1.2.1. Standard Gibbs free energy of reaction for methane pyrolysis.

Reaction of methane with oxygen results in a completely different picture (Figure 1.2.2). The conversion of methane into ethylene is thermodynamically favoured at much lower temperatures by the presence of oxygen. However, carbon oxide formation is favoured even more, which makes it also a challenge to control the hydrocarbon production kinetically. One way of controlling the product formation is by the use of catalysts. Since the first catalytic systems have been reported (1982) much progress has been made in catalyst development resulting in quite active and selective catalysts. The next paragraph will describe the most important trends in catalyst development for the oxidative coupling of methane.

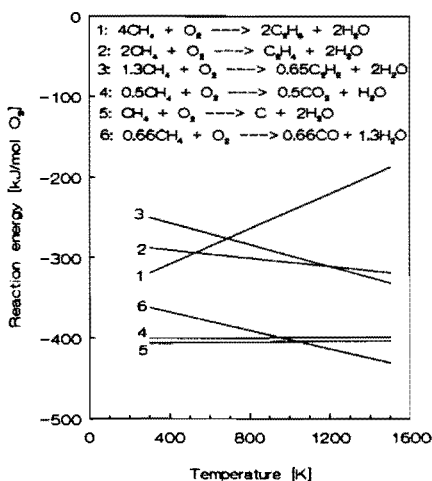


Figure 1.2.2. Standard Gibbs free energy of reaction for the reaction of methane with oxygen.

1.3 LITERATURE SUMMARY

Quite a number of catalyst systems have been reported for oxidative coupling of methane during the last 10 years⁶. Roughly, the catalyst systems can be divided into three groups: reducible metal oxides, irreducible metal oxides and rare earth metal oxides. The first catalyst systems reported belonged to the reducible metal oxides. They were operated not as true catalysts, but as oxygen transfer agents in a cyclic mode of operation in which methane and air were successively fed over the catalyst at ambient pressures. In 1978 Mitchell and Wagborne (Exxon Research & Engineering Co., USA)⁷ reported Pt on carriers like MgAl_2O_3 or BaAl_2O_3 as a catalyst system for the conversion of methane into C_{2+} hydrocarbons at 600 to 700°C. They claimed a C_{2+} yield of 25.4% (C_{2+} selectivity ($s_{\text{C}_{2+}}$) = 57%), of which the largest part consisted of C_6H_6 (32%).

Related to this work was the work of Fang et al.⁸ They investigated the catalytic methane pyrolysis reaction and found $\text{ThO}_2/\text{SiO}_2$ as an active and selective catalyst for the methane conversion into C_{2+} (Yield C_{2+} = 3.15%). They claimed that most of the ethane was produced by coupling of methyl radicals in the gas phase.

In 1982 Keller and Bhasin⁹ published the results of extended catalyst testing in a cyclic mode of operation. They tested various metal oxides at 700° to 900°C and found Bi, Sb, Sn, Pb, Ta, Mn and Cd supported on Al_2O_3 as materials which showed the highest activity for C_{2+} hydrocarbon formation. Workers at the Atlantic Richfield Company (ARCO, USA) carried out analogous experiments, which resulted in various patents¹⁰ claiming catalysts suitable for methane conversion into C_{2+} hydrocarbons via the cyclic mode of operation. These catalyst included supported oxides of Mn, In, Sb, Sn, Bi, Pb¹¹. The best catalyst system found was 5% $\text{Na}_4\text{P}_2\text{O}_7$ /15%Mn/ SiO_2 with which C_{2+} yields of 20% were achieved ($s\text{C}_{2+}$ = 70%)¹². Keller and Bhasin also tested their catalysts in the cofeed mode of operation in which methane and oxygen were fed simultaneously to the reactor. This resulted in a decrease of C_{2+} selectivity mainly due to total oxidation reactions catalyzed by the stainless steel reactor wall. Change of the reactor wall to quartz eliminated this unwanted catalytic effect.

Hinsen and Baerns¹³ were the first to report on the truly catalytic reactions of methane with oxygen (cofeed mode) with good selectivity and activity. A $\text{PbO}/\text{Al}_2\text{O}_3$ catalyst resulted in a C_{2+} yield of 4.3% with C_{2+} selectivity of 58%. The serious disadvantage of this catalytic system appeared to be the volatilization of the PbO at the reaction temperatures of 750° resulting in a rapid deactivation.¹⁴

The second group of catalysts comprises alkali - alkaline earth metal oxides which are irreducible under normal catalytic reaction conditions. Fox et al.¹⁵ reported good results with Na/CaO for the cyclic mode of operation. They attributed the working of this catalyst system to the super basicity of alkali - alkaline combinations. Ito et al.¹⁶ (from the group of Lunsford, A&M University, Texas, USA) reported excellent coupling results (C_{2+} yield = 19%) with Li doped MgO . Ito claimed Li^+O^- centres as the reactive centres for methane activation. These centres are stabilized in the MgO matrix, because Li^+ ions fit exactly at the lattice site normally occupied by Mg^{2+} . Analogous combinations also appear active and selective for methane conversion e.g. Na/CaO , K/BaO ¹⁷.

The third group of catalysts comprises the rare earth metal oxides first reported by Otsuka et al.¹⁸ Sm_2O_3 and Dy_2O_3 appeared to be the most promising systems for methane conversion into ethane and ethylene (C_{2+} = yield 12.4%, $s\text{C}_{2+}$ = 41.2%). Otsuka further discovered that doping of these catalysts with alkali carbonates resulted in even better coupling performances¹⁹ (C_{2+} yield = 22.3%, $s\text{C}_{2+}$ = 54.1%). Doping with LiCl improved the ethylene yield significantly. This is due to the interaction of chlorine radicals which are very effective in methane activation²⁰. The highest C_{2+} yield (30.6% at $s\text{C}_{2+}$ = 64.7%) reported was achieved with $\text{LiCl}/\text{Mn-oxide}$ ²¹. However, this catalyst rapidly deactivated due to the loss of the chlorine. Also this yield was achieved at very diluted conditions. Without dilution of the gas phase with helium the C_{2+} yield dropped

to 15.7% (sC_{2+} = 48.9%). Table 1.3.1 summarizes the important catalyst systems reported for oxidative coupling of methane in the cofeed mode of operation.^{22 23 24 25} Most of the catalysts maintain their reported optimal C_{2+} yields only for a limited time and deactivate rather rapidly.

Of the reported catalyst systems Li doped MgO, first reported by the Lunsford group, belongs to one of the best catalyst systems with high C_{2+} selectivity (>65%) at high C_{2+} yields. In 1986 when we started this investigation Li doped MgO was certainly the best choice for further study and optimization.

Concerning the nature of the active site for methane activation, contradictions still need to be solved. Most investigations concern the Li/MgO catalyst, which will be discussed first. As already mentioned, Li^+O^- centres have been proposed by Ito et al.¹⁶ as the reactive sites for methane activation.

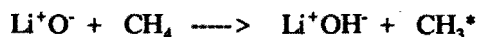
Table 1.3.1. Results of various catalyst systems used for oxidative coupling of methane in cofeed mode.

| Catalyst system | C_{2+} Yield (%) | C_{2+} Sel (%) | P_{inert}/P_{tot} | Temp. (K) | Ref. |
|--|--------------------|------------------|---------------------|-----------|-----------|
| PbO/Al ₂ O ₃ | 4.3 | 58 | 0.33 | 1023 | 13 |
| 15%Mn5%Na ₄ P ₂ O ₇ /SiO ₂ | 14.5 | 66 | 0.40 | 1173 | 27 |
| 12.5% NaMnO ₄ /SiO ₂ | 15.7 | 70 | 0.40 | 993 | 27 |
| 3%Li/MgO | 18.4 | 50 | 0.57 | 993 | 22, 26 |
| 7%Li/MgO | 15 | 65 | 0.40 | 1073 | This work |
| 10%Li/CaO | 25.9 | 53 | 0.96 | 1073 | 25 |
| Na/MgO | 22.4 | 57 | 0.96 | 1073 | 23 |
| K/BaO | 20.2 | 42 | 0.96 | 1073 | 17 |
| Sm ₂ O ₃ | 12.4 | 41 | 0.93 | 1023 | 19 |
| LiCl/Sm ₂ O ₃ | 19.9 | 69 | 0.93 | 1023 | 19 |
| LiCl/Mn-oxide | 30.6 | 65 | 0.93 | 1023 | 21 |
| Li/ZnO | 18 | 61 | 0 | 1013 | 24 |

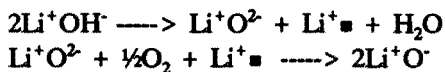
These centres are created in the presence of gas phase oxygen at high temperatures via migration of Li^+ into the MgO lattice. The Li^+ ions replace the Mg^{2+} cations or vacancies. In order to maintain charge neutrality the substitutional Li^+ ions capture holes (■) provided by the dissociation of di-oxygen through the following process:



The Li^+O^- sites react with CH_4 releasing methyl radicals into the gas phase:

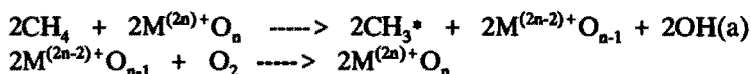


The reoxidation of the active site is believed to proceed via the following scheme:



Roos et al.²⁶ suggested, contradictory to Ito, that a weakly bonded di-atomic oxygen species was responsible for the methane activation over Li/MgO. This suggestion was based on kinetic investigations. The active sites might be created on the surface of Li/MgO by gradual loss of CO₂ from lithium carbonate species in the presence of gas phase oxygen. This reaction mechanism will be discussed in detail in Chapter 3.

For the reducible metal oxide catalysts a Mars - Van Krevelen kind of reaction mechanism is believed to be applicable.^{27,28} Methane is activated by the lattice oxygen, which is removed from the lattice as water. This site is filled again with gas phase oxygen:



For the third group of catalysts, the rare earth metal oxides, Otsuka²⁹ suggested a di-atomic oxygen species as the active oxygen species based on kinetic investigations. Lin et al.³⁰ detected O₂⁻ ions as the dominant species on the catalyst surface of La₂O₃. Together with these species they detected a lot of methyl radicals in the gas phase. On the other hand Lee and Oyama⁶ speculate that an O⁻ species could still be the active oxygen species, because the O⁻ species cannot be detected by EPR spectroscopy, because the resting form is the dimer O₂⁻ species.

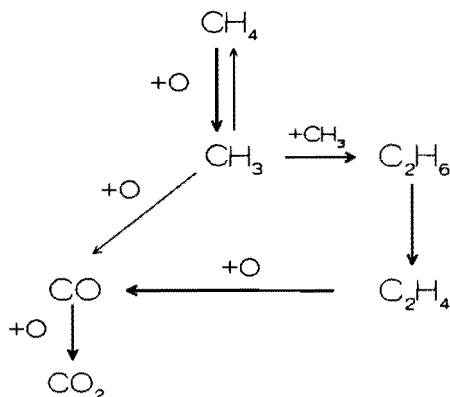


Figure 1.3.1. Reaction scheme for oxidative coupling of methane.

Most of the mechanistic publications in the literature agree on the occurrence of methyl radicals. They play the key role in the formation of C_{2+} hydrocarbons and total oxidation products. The important reaction steps of the methane coupling process can be summarized by the scheme shown in Figure 1.3.1. Dependent on the catalyst system and the process condition the direct oxidation of methane to CO_x products may be insignificant or quite important. Over Li/MgO this reaction plays a minor role. Main primary product is ethane, which is dehydrogenated to ethylene. The ethylene is subjected to further oxidation, inevitably leading to CO_x . Much discussion takes place concerning the role of homogeneous (gas phase) and heterogeneous (catalytic) reactions in the reaction mechanism. Still, the relative importance of surface and gas phase reactions has received only little attention in literature. Labinger et al.³¹ reported the predominance of gas phase reactions in the reaction mechanism of methane coupling over $NaMnO_4/MgO$ at temperatures above $800^\circ C$. Generally, it has become accepted that above $800^\circ C$ gas phase reactions are dominating. However, based on the striking resemblance between product selectivity patterns reported in the presence of a catalyst and those obtained in an empty tube a common type of branched chain propagation may be responsible for the overall product selectivity in the system despite the difference in initiation reactions³².

We have shown that the product selectivity of the oxidative coupling of methane over Li/MgO can be simulated by adapting the initiation reaction in a kinetic model describing the homogeneous gas phase oxidative coupling. The role of the catalyst may thus be restricted to that of a methyl radical producer increasing the methyl radical concentration in the gas phase³³ (Chapter 5).

The simultaneous occurrence of homogeneous gas phase and heterogeneous catalytic reactions seriously complicates the study of the catalytic methane oxidation process. An impression of the importance of homogeneous gas phase reactions can be obtained from catalytic experiments at strongly reduced pressures. This reduces the reaction rates and increases the contribution of heterogeneous relative to homogeneous reactions. In Chapter 4 low pressure experiments are used to determine the relationship between the surface and the gas phase reactions.

Kinetic investigations are complicated by the occurrence of heterogeneous and homogeneous reactions at the same time. A point of discussion is the presence or the absence of methane adsorption. Labinger and Ott³⁴ claimed a Rideal type of mechanism wherein methyl radicals are produced at the oxide surface and hydrocarbon formation takes place in the gas phase. On the other hand Otsuka and Jinno²⁹ claimed a Langmuir - Hinshelwood type of mechanism involving CH_4 and O_2 adsorption on different sites over Sm_2O_3 to be applicable, which was based on kinetic measurements. The methane adsorption on Sm_2O_3 was confirmed by Ekstrom and Lapszewicz³⁵ by isotopic pulse experiments. Roos et al.^{22, 26} found a Langmuir - Hinshelwood type of mechanism to be suitable also for Li/MgO at $720^\circ C$. Iwamatsu and Aika³⁶ could not discriminate between a Rideal and a Langmuir - Hinshelwood type of mechanism for methane coupling over

Na/MgO. They proposed the Rideal mechanism as more likely. In Chapter 3 experiments are described, which elucidate the occurrence of methane adsorption on Li/MgO by the so-called steady-state isotopic transient kinetic analysis (SSITKA) technique. It is shown that methane adsorption on Li/MgO is not significant compared to oxygen adsorption. Based on this, a Rideal type of mechanism is selected to describe the kinetics (Chapter 5).

Geerts et al³ have carried out an economic evaluation study for the production of ethylene from natural gas via oxidative coupling. This process was compared to a conventional process for ethylene production: naphtha cracking. Three different kind of reactor types were compared: a multi-tubular, a multi-stage and a fluidized bed reactor. The fluidized bed reactor seems the most suitable one, mainly due to its superior heat transfer properties. The oxidative coupling of methane into ethylene appears to be a profitable process, when a C_{2+} yield of 25% is possible at a C_{2+} selectivity of at least 65%.

Edwards and Tyler³⁷ confirmed the performance of the fluidized bed reactor experimentally using Li doped MgO. They also considered the simultaneous conversion of ethane into ethylene a key factor in favour of the use of the fluidized bed reactor. We have also shown that cracking of ethane into ethylene can be effectively integrated into the coupling process.³⁸ The post-catalytic space of the coupling reactor can act as an ethane cracker running on the energy produced in the coupling process. Edwards and Tyler concluded that the catalyst development should be aimed at 25-30% methane conversion with a C_{2+} hydrocarbon selectivity of 75-80%. Kuo et al.³⁹ compared the indirect route of conversion of natural gas into hydrocarbons via synthesis gas and methanol to the direct conversion route. They concluded that a methane conversion of 35% at 88% C_{2+} selectivity is required for an attractive process. However, they did not evaluate the economics of the process, but only the thermal efficiencies.

Summarizing it can be concluded that the catalytic oxidative coupling of methane is a very promising process with a high potential, but that the catalyst performances still need improvement to get catalysts which are suited for a commercial process. Therefore, further research is necessary.

1.4 AIMS AND OUTLINE OF THIS THESIS

The catalytic oxidative coupling of methane is a promising, new route for the conversion of natural gas into hydrocarbons. Methane is converted directly into ethylene by partial oxidation. This is an attractive alternative for the indirect route which comprises the cumbersome and energetically unfavoured production of synthesis gas via steam reforming of methane and the Fischer - Tropsch process to produce hydrocarbons.

This thesis is focussed on the catalytic oxidative coupling of methane with Li doped

MgO. Aim is to achieve a better understanding of the oxidative coupling process, the working principle of the Li/MgO catalyst and the reaction mechanism.

Chapter 2 deals with the influence of the catalyst preparation method and the catalyst pretreatment on the C_{2+} hydrocarbon production. Especially the influence of the lithium salt, used for the Li/MgO catalyst synthesis and the influence of oxygen pretreatment were investigated.

Chapter 3 describes the catalyst deactivation mechanism. The interaction of methane and oxygen with the Li/MgO catalyst is investigated by means of the so-called steady-state isotopic transient kinetic analysis (SSITKA) technique with labelled methane ($^{13}CH_4$) and labelled oxygen ($^{18}O_2$). This resulted in a model for the working principle of the catalyst.

Chapter 4 is focussed on the elucidation of the important reaction steps and the mechanism of the methane conversion into ethylene. Experiments at reduced total pressure are described, which reveal the interaction of homogenous and heterogeneous reaction steps. Admixing experiments with methane/ethane/oxygen and methane/ethylene/oxygen mixtures elucidate the relative reactivity of methane, ethane and ethylene over Li/MgO. Based on these reactivities it is shown that the C_{2+} yield over Li/MgO is restricted to a maximum.

As radicals, especially methyl radicals, play an important role in the reaction mechanism the interaction of radicals with Li/MgO could be important. By means of an alternative radical source: a glow discharge in argon, the influence of Li/MgO on radical reactions is investigated.

Chapter 5 describes kinetic investigations in which the influence of methane and oxygen pressure on the product selectivity is determined. The product selectivity of the catalytic oxidative coupling of methane is described by a consecutive model in which methane is converted mainly to ethane, ethane to ethylene and ethylene to CO_x .

Chapter 6, finally, gives general conclusions and perspectives for the future development of catalysts suitable for the oxidative coupling of methane.

REFERENCES

1. Essobron, november (1989).
2. M.J. van der Burgt, J. van Klinken, S.T. Sie, The SHELL Middle distillate Process, Selected Papers, SHELL, London, November (1985).
3. J.W.M.H. Geerts, J.H.B.J. Hoebink and K. van der Wiele, ACS Meeting, Boston, April (1990).
4. L. Devries, P.R. Ryason, U.S. Patent, 4507517 (1985).
5. G.P. van der Zwet, P.A.J.M. Hendriks and R.A. van Santen, Catal. Today, 4, 365 - 369 (1989).
6. J.S. Lee and S.T. Oyama, Catal. Rev. -Sci. Eng., 30(2), 249 -280 (1988).
7. H.L. Mitchell and R.H. Wagborne, US Patent no. 4205194, (1980); US Patent no. 4239658 (1980).
8. T. Fang and C.T. Yeh, J. Chin. Chem. Soc., 29, 263-273 (1981).

9. G.E. Keller and M.M. Bhasin, *J. Catal.*, 73, 9 (1982).
10. C.A. Jones, J.J. Leonard and J.A. Sofranko, US patents no. 4443644 to 4443649 and no 4444984 (1984).
11. J.A. Sofranko, J.J. Leonard and C.A. Jones, *J. Catal.*, 103, 302 (1987).
12. C.A. Jones and J.A. Sofranko, World Patent, WO 85/00804 (1985).
13. W. Hinsen and M. Baerns, *Chem. Ztg.* 107, 223 (1983).
14. J.A. Roos, A.G. Bakker, H. Bosch, J.G. van Ommen and J.R.H. Ross, *Catal. Today*, 1, 133 (1987).
15. J.R. Fox, B.S. Curatolo and F.A. Pesa, US Patent no 4450310 (1984).
16. T. Ito, J-X Wang, C.H. Lin and J.H. Lunsford, *J. Am. Chem. Soc.*, 107, 5062- 5068 (1985).
17. K. Aika, T. Moriyama, N. Takasaki and E. Iwamatsu, *J. Chem. Soc., Chem. Commun.*, 1210 (1986).
18. K. Otsuka, K. Jinno and A. Morikawa, *Chem. Lett.*, 499 (1985).
19. K. Otsuka, Q. Liu and A. Morikawa, *J. Chem. Soc., Chem. Commun.*, 586 (1986).
20. S.W. Benson, US Patent no. 4199533 (1980).
21. K. Otsuka and T. Komatsu, *J. Chem. Soc., Chem. Commun.*, 388 (1987).
22. J.H. Koits and J.H. Lunsford, European Patent no 0196541 (1986).
23. E. Iwamatsu, T. Moriyama, N. Takasaki and K. Aika, *J. Catal.*, 113, 25 -35 (1988).
24. T. Doi, Y. Utsumi and I. Matsuura, *Proceedings 9th Int. Congr. on Catal.*, Eds M.J. Phillips and M. Ternan, Calgary, Canada, 2, 937 - 943 (1988).
25. T. Ishiyama, T. Watanabe and K. Aika, *Catal. Today*, 6, 391 - 398 (1990).
26. J.A. Roos, S.J. Korf, R.H.J. Veehof, J.G. van Ommen and J.R.H. Ross, *Appl. Catal.*, 52, 131 (1989).
27. J.A. Sofranko, J.J. Leonard, C.A. Jones, A. Gaffney and H.E Withers, *Preprints Symposium on Hydrocarbon Oxidation, The Division of Petroleum Chemistry, INC. Am. Chem. Soc., New Orleans Meeting, August 30 - September 4 (1987).*
28. K. Asami, T. Shikada, K. Fujimoto and H. Tominaga, *Ind. Eng. Chem. Res.*, 26, 2348 - 2353 (1987).
29. K. Otsuka and K. Jinno, *Inorg. Chim. Acta.*, 121, 237 (1986).
30. C-H Lin, K.D. Campbell, J-X Wang and J.H. Lunsford, *J. Phys. Chem.*, 90, 534 (1986).
31. J.A. Labinger, S. Mehta, K.C. Ott, H.K. Rockstad and S. Zoumalan, *J. Catal.*, 513 (1988).
32. O.T. Onsager, R. Lodeng, P. Soraker, A. Amundskaas and B. Helleborg, *Catal. Today*, 4, 355 -363 (1989).
33. J.M.N. van Kasteren, J.W.M.H. Geerts and K. van der Wiele, *Proceedings 1st World Congress, New Developments in Selective Oxidation, Ed. G. Centi & F. Trifiro, Rimini, Italy, 18 - 22 september 1989, Stud. Surf. Sci. Catal.*, 55, 343 - 352 (1990).
34. J.A. Labinger and K.C. Ott, *J. Phys. Chem.*, 91, 2682 - 2684 (1987).
35. A. Ekstrom and J.A. Lapszewicz, *Preprints Symposium on Direct Methane to Higher Homologues, The Division of Petroleum Chemistry, INC., Am. Chem. Soc., Los Angeles Meeting, Sep. 25 - 30 (1988).*
36. E. Iwamatsu and K. Aika, *J. Catal.*, 117, 416-431 (1989).
37. J.H. Edwards and R.J. Tyler, *Catal. Today*, 4, 345 - 354 (1989).
38. J.M.N. van Kasteren, J.W.M.H. Geerts and K. van der Wiele, *Proceedings 9th Int. Congr. on Catal.*, Eds. M.J. Phillips and M. Ternan, Calgary, Canada, 2, 930 - 936 (1988).
39. J.C.W. Kuo, C.T. Kresge and R.E. Palermo, *Catal. Today.*, 4, 463 - 470 (1989).

CHAPTER 2

Li/MgO CATALYST PREPARATION AND PERFORMANCE

2.1 INTRODUCTION

Li doped MgO appeared to be a very good catalytic system for the oxidative coupling of methane. Ito et al.¹ reported C_{2+} yields up to 19% for Li/MgO in a continuous process. They prepared Li/MgO by stirring and heating a slurry of Li_2CO_3 and MgO in water until a thick paste remained. The paste was then air-dried over night at 140°C. The Li_2CO_3 /MgO thus obtained was converted to Li promoted MgO at 465°C for 1 hour under an oxygen flow of 0.83 ml/s. Based on this preparation recipe we developed our own preparation method and investigated the influence of this method on the catalytic performance in a continuous methane activation process.

Driscoll et al.² proposed Li^+O^- centres stabilized in the MgO matrix as the centres responsible for the high activity and selectivity in the methane activation process. These centres were formed in Li/MgO at high temperatures in the presence of gas phase oxygen. According to his theory an oxygen pretreatment of the catalyst would be beneficial for the catalytic performance. The influence of an oxygen pretreatment on the performance of the Li/MgO catalyst was investigated by carrying out experiments in which the catalyst was heated to the reaction temperature under a flow of helium and brought into contact with a flow of an oxygen-helium mixture prior to reaction.

2.2 CATALYST PREPARATION AND CONTINUOUS OXIDATION EQUIPMENT

The experiments described in this chapter were carried out in a continuous flow oxidation set-up operated at atmospheric pressure³. This laboratory set-up can be divided into three parts: the feed section, the reactor section and the analytical section (Figure 2.2.1). The heart of the setup is a quartz micro fixed bed reactor (Figure 2.2.2). This reactor contained a quartz porous filter to carry the catalyst and a quartz thermocouple tube which prevents the occurrence of undesired catalytic oxidation reactions at a steel or metal surface as reported by Keller and Bhasin⁴.

After heating up of the catalyst (typically 0.5 g) to the desired reaction temperature (typically 800 °C) under a flow of helium, the reaction gas was introduced. The flow rate was adjusted with separate mass flow controllers (Hitec) (typically 50-500 Nml/min) for methane (Hoekloos 99.6%), oxygen (Hoekloos 99.9%) and helium (Hoekloos >99.995%). Oxygen pretreatment experiments consisted of flushing the catalyst (at the reaction temperature (800 °C)) with artificial air (He 80%, O₂ 20%) during a variable

number of minutes followed by a flush (5 minutes) with pure helium to remove all the excess oxygen. After the pretreatment the reaction was carried out under standard conditions ($T = 800^\circ\text{C}$, $W/F = 300 \text{ g.s./l.}$ $\text{CH}_4/\text{O}_2 = 5$, $\text{CH}_4/\text{He} = 1.25$)

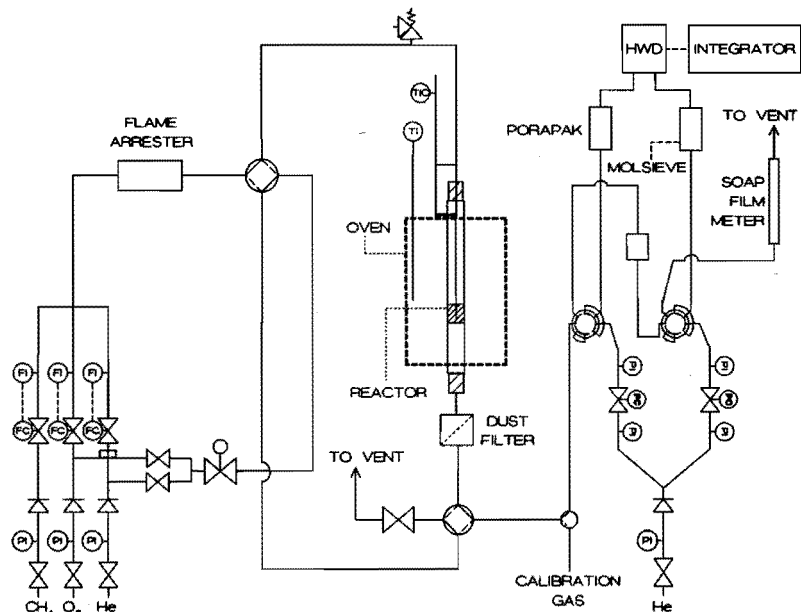


Figure 2.2.1. Flow scheme of the micro flow reactor set-up.

The product gases were analyzed by gas chromatography. The column packings were Porapak R (3m) for the separation of CH_4 , CO_2 , C_2H_4 , C_2H_6 , C_3H_6 , C_3H_8 and H_2O and a 5-A molecular sieve (3m) for the separation of H_2 , O_2 , CH_4 and CO . The porapak was operated at 70°C and the molecular sieve at 110°C . Both columns were connected to a Thermal Conductivity Detector (TCD) in a Carlo Erba 4300 gaschromatograph with helium as the carrier gas. The analysis was carried out automatically with the aid of two pneumatically controlled sampling valves. A complete product analysis needed about 20 min. With this method a carbon balance of at least 98% was achieved.

The different Li doped MgO catalysts were made by heating a slurry of a lithium salt and MgO in water until a thick paste remained. The quantities of the lithium salt and the MgO were calculated to produce a 7 wt% $\text{Li}/(\text{Li} + \text{MgO})$ catalyst. The paste was dried at 120°C for 24 hours.

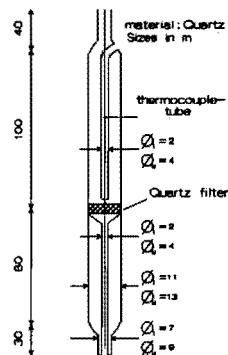


Figure 2.2.2. Quartz micro fixed bed reactor.

Finally the catalyst was calcined at 900°C for 4 hours, crushed and sieved to the desired particle size (preferably 0.4-0.6 mm). The high calcination temperature assured that no additional sintering could occur under the reaction conditions applied. In contrast with the preparation method of Ito et al.¹, who calcined the catalyst in the reactor just before the start-up of the reaction, we know the catalyst weight under reaction conditions.

Figure 2.2.3. depicts the pore size distribution graph of a $\text{Li}_2\text{CO}_3/\text{MgO}$ catalyst as measured by the mercury penetration method. It can be seen clearly that the catalyst does not contain any pores below 1000 Å. At 900°C almost complete sintering has occurred resulting in a specific surface area of less than $1 \text{ m}^2/\text{g}$. The main cause of the sintering is the Li_2CO_3 phase which melts above 723°C.

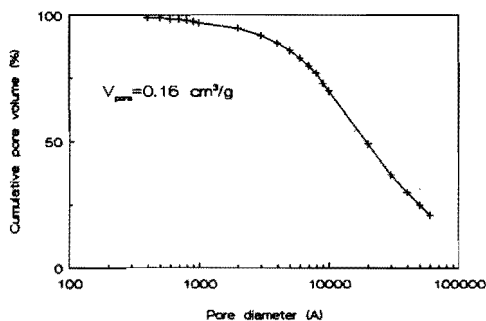


Figure 2.2.3. Pore diameter of a fresh Li/MgO catalyst measured by mercury penetration method.

2.3 INFLUENCE OF CATALYST PREPARATION ON THE COUPLING PERFORMANCE

Li/MgO catalysts with a lithium content of 7 wt% $\text{Li}/(\text{Li} + \text{MgO})$ were prepared from different lithium salts and magnesium oxide. The use of different lithium salts can result in catalysts with different structure and with different catalytic properties⁵. Table 2.3.1 shows the various catalysts prepared and their pore volume as determined by the mercury penetration method.

From Table 2.3.1 it is clear that the lithium nitrate catalyst has the highest pore volume; much higher than all other catalysts prepared. As a result the surface area is much higher. Therefore, the methane conversion is also expected to be much higher. The LiF/MgO catalyst was the only catalyst, which did not contain the Li_2CO_3 phase after calcination as measured by XRD. LiF is stable up to 930°C while the other salts decompose to Li_2O (at 900°C). Li_2O is not stable at room temperature in the presence of gas phase CO_2 ; it rapidly reacts to Li_2CO_3 . Starting the catalyst preparation with a lithium salt, which decomposes at temperatures below 900°C to Li_2O will always result

in a $\text{Li}_2\text{CO}_3/\text{MgO}$ catalyst, when exposed to CO_2 at lower temperatures. Therefore, the difference between the differently prepared Li/MgO catalysts (except LiF/MgO) can be reduced to differences in pore structure, lithium content and lithium dispersion.

Table 2.3.1. Li/MgO catalysts and their pore volume after calcination at 900°C .

| Starting Salts | Pore Volume (ml/g) |
|-------------------------------------|--------------------|
| $\text{Li}_2\text{CO}_3/\text{MgO}$ | 0.018 |
| LiNO_3/MgO | 0.164 |
| LiOH/MgO | 0.012 |
| LiF/MgO | 0.018 |

All catalysts prepared were tested in a micro fixed bed reactor at 800°C with a continuous feed of methane (50 Nml/min), oxygen (10 Nml/min) and helium (40 Nml/min). The contact time (W/F) was 300 g.s/l and the methane/oxygen ratio was 5.

Figure 2.3.1 shows the methane and oxygen conversion as a function of the time on stream (h) for three different Li/MgO catalysts.

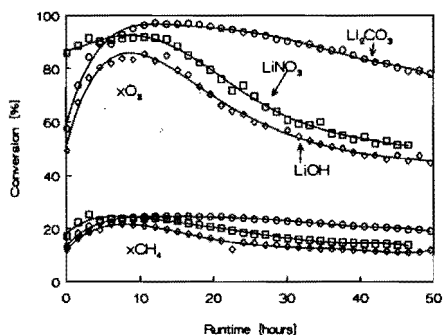


Figure 2.3.1. Methane and oxygen conversion as function of time on stream for different Li/MgO catalyst. $T=800^\circ\text{C}$, $\text{CH}_4/\text{O}_2=5$, $\text{W}/\text{F}=0.3$ g.s/ml.

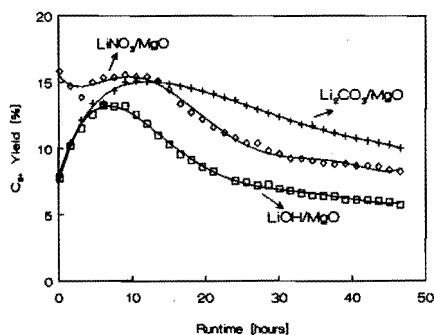


Figure 2.3.2. C_{2+} yield as function of time on stream for different Li/MgO catalysts. $T=800^\circ\text{C}$, $\text{CH}_4/\text{O}_2=5$, $\text{W}/\text{F}=0.3$ g.s/ml.

The LiF/MgO catalyst could not be measured for a long time, because the reactor broke during the first hour of the experiment. The fluoride is very aggressive towards the quartz glass and destroys its structure. Its initially measured activity and C_{2+} selectivity were very poor. This indicates that lithium added as lithium fluoride does not lead to an active and selective catalyst. Apparently lithium fluoride is too stable to allow the lithium ion to be integrated in the magnesium oxide and form active centres like Li^+O^- .

During reaction time the oxygen conversion shows a maximum (Figure 2.3.1). This is typical for the Li/MgO catalysts calcined at temperatures higher than the reaction temperature. The Li/MgO catalysts calcined at temperatures lower than the reaction temperature show a decrease in activity from start-up of the reaction.¹ This behaviour is mainly caused by a sintering process. Li/MgO catalysts, which have been calcined at temperatures much higher than the reaction temperature are already completely sintered before the start-up of the reaction. However, striking is that the activity of a high temperature calcined catalyst increases during the first hours on stream. This can only mean that more active centres are created during reaction.

The catalyst morphology influences the catalytic behaviour. As expected the lithium nitrate catalyst has the highest initial activity. However, a much more pronounced performance was expected, with respect to the porosity data. Instead the $\text{Li}_2\text{CO}_3/\text{MgO}$ catalyst reached an even higher activity level and showed a much slower deactivation, once the first 8 hours were passed.

A comparison of performance between the different catalysts can best be done by plotting the C_{2+} yields versus time on stream. This is shown in Figure 2.3.2. The LiNO_3/MgO catalyst maintains a C_{2+} yield of 15% for 10 hours, but then rapidly deactivates. The $\text{Li}_2\text{CO}_3/\text{MgO}$ has a better stability in time, probably due to its lower surface area. Summarizing it can be said that the catalyst preparation method influences the course of the activity, especially during early reaction times, but that the differences in coupling performance in time diminish. All the Li/MgO catalysts deactivate to more or less the same performance level. This suggests that the same deactivation mechanism is applicable to the different Li/MgO catalysts (see also Chapter 3).

2.4 THE INFLUENCE OF CATALYST PRETREATMENT ON THE COUPLING PERFORMANCE

As mentioned in chapter 1 the active centres in Li/MgO (Li^+O^-) are believed to be created via migration of Li^+ ions into the MgO lattice in the presence of gas phase oxygen. According to Driscoll et al.² the gas phase oxygen is adsorbed and built into the lattice. A pretreatment of the catalyst with gas phase oxygen increases the amount of active centres formed and should therefore influence the catalytic activity. This is investigated by carrying out experiments in which the Li/MgO catalyst was pretreated with and without oxygen, previous to start-up of the reaction. The Li/MgO catalyst used was prepared from Li_2CO_3 and MgO as described in paragraph 2.2. The reaction conditions used were the standard reaction conditions (paragraph 2.2).

Figure 2.4.1 shows the methane and oxygen conversion as a function of the reaction time for different oxygen pretreatment times. It shows that the methane conversion (activity) increases with increasing oxygen pretreatment time. A longer oxygen pretreatment time means a higher initial activity, in agreement with Driscoll's theory.

The catalyst with the longest oxygen pretreatment time (900 min.) shows an increased activity (methane conversion) during the whole experiment as compared to the catalysts with the short pretreatment times. An oxygen pretreatment of the catalyst prior to the start-up of the reaction is indeed beneficial for the activity of the catalyst. The influence of the oxygen pretreatment time on the product selectivity can be shown by plotting the C_{2+} yield as function of the reaction time.

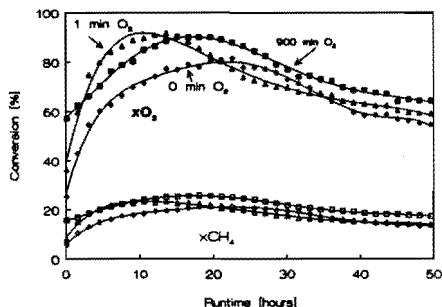


Figure 2.4.1. Methane and oxygen conversion as function of time on stream for different oxygen pretreatment times.

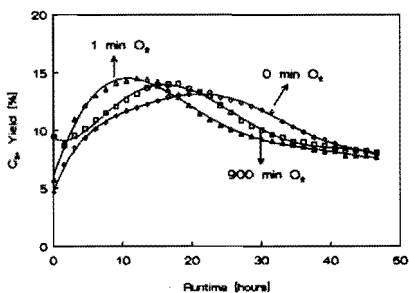


Figure 2.4.2. C_{2+} yield as function of time on stream for different oxygen pretreatment times.

Figure 2.4.2 shows the influence of the oxygen pretreatment on the C_{2+} yield. Clearly, an oxygen pretreatment is beneficial for the C_{2+} yield, because no pretreatment results in a lower maximum C_{2+} yield. However, after 20 hours the catalyst with the longest pretreatment time (the most active one) has a lower C_{2+} yield than the catalyst without any oxygen pretreatment. This means that the oxygen pretreatment lowers the C_{2+} selectivity. The longer the oxygen pretreatment time the more the C_{2+} selectivity is lowered. Therefore, there exists an optimal oxygen pretreatment time: this optimal pretreatment causes an increase in activity without a great loss in C_{2+} selectivity resulting in the highest C_{2+} yield. Concluding it can be stated that an oxygen pretreatment of the Li/MgO catalyst prior to the start-up of the reaction results in a more active, but less selective, coupling catalyst.

2.5 CONCLUSIONS

The catalyst structure has an influence on the activity and selectivity. The same preparation method gives, starting with different lithium salts and magnesium oxide, in

principle the same catalyst concerning the phases existing : lithium carbonate and magnesium oxide.

The Li/MgO catalysts calcined at temperatures higher than the reaction temperature do not show a stable catalytic performance during the first 50 hours on stream. The catalyst synthesis method influences the C_{2+} yield, which can be reached. The $LiNO_3/MgO$ catalyst has a high pore volume and a large surface area compared to the other prepared Li/MgO catalyst. This appears to be favourable for the coupling reactions: a stable C_{2+} yield of 15% for 10 hours. However, deactivation of this catalyst is also quite fast. Due to the higher surface area the active component apparently gets lost more easily. The differently prepared Li/MgO catalysts deactivate all more or less to the same activity level indicating that the same deactivation mechanism is applicable for all Li/MgO catalysts prepared.

An oxygen pretreatment of the Li/MgO catalyst is favourable for the activity of the catalyst, but not for the C_{2+} selectivity. There seems to exist an optimal oxygen pretreatment time with respect to the maximum achievable C_{2+} yield.

REFERENCES

1. T. Ito, J.X. Wang, C.H. Lin and J.H. Lunsford, *J.Am.Chem.Soc.*, 107, 5062-68 (1985).
2. D.J. Driscoll, W. Martir, J.X. Wang and J.H. Lunsford, *J.Am.Chem.Soc.*, 107, 58-63 (1985).
3. J.M.N. van Kasteren, J.W.M.H. Geerts and K. van der Wiele, *Proceedings 9th Int. Congr. Catal. (ICC)*, Calgary, Canada, 2, 930-936 (1988).
4. G.E. Keller and M.M. Bhasin, *J. Catal.*, 73, 9-19 (1982).
5. K. Otsuka, Q Liu, M. Hatano and A. Morikawa, *Chem. Lett.*, 467-468 (1986).

CHAPTER 3

CATALYST DYNAMICS AND DEACTIVATION MECHANISM

3.1 INTRODUCTION

Essential for a catalytic process is not only the activity and selectivity of the catalyst, but especially the lifetime of a catalyst. The economics of a catalytic process often depend strongly on the catalyst stability. In Chapter 2 it became clear that the Li/MgO catalyst did not show a stable coupling performance during the first 50 hours on stream. It is the purpose of this chapter to elucidate the mechanisms on which this unstable behaviour is based. This was done by monitoring the lithium loss of the Li/MgO catalyst as function of the time on stream and determine the influence of reactant gases on this lithium loss.

The stability of the catalytic performance of the Li/MgO catalyst was investigated by determining the influence of changes in process conditions and gas composition on the catalytic behaviour under a standard set of reaction conditions.

The working principle of this catalyst was investigated by using the steady-state isotopic transient kinetic analysis (SSITKA) technique with which it is possible to determine the number of exchangeable oxygen atoms. These experiments give new insights into the catalytic mechanism which is occurring under steady state reaction conditions.

3.2 EXPERIMENTAL

The Li/MgO catalyst used was prepared with Li_2CO_3 and MgO as starting salts according to the method described in paragraph 2.2. The lithium content of the Li/MgO catalysts prepared was measured by flame emission spectroscopy¹. The experiments to determine the catalyst stability and its deactivation behaviour were carried out in the continuous oxidation equipment described in Chapter 2.

For the SSITKA experiments a special set-up was designed and built (Figure 3.2.1). With this set-up it is possible to create two chemically identical gas mixtures consisting of e.g. $\text{CH}_4/^{16}\text{O}_2/\text{He}$ and $\text{CH}_4/^{18}\text{O}_2/\text{He}$ with a typical total flow rate of 100 Nml/min each. The isotope was fed to the system from a lecture bottle. The two gas mixtures were fed to the reactor via the 4 way valve K1, which makes it possible to switch instantaneously. The catalyst (typically 0.25 g) was placed on a porous filter in the quartz reactor (Figure 2.2.2.) and the remaining dead volume was filled with quartz particles in order to eliminate back mixing effects. Under typical flow conditions at 800°C with a flow-rate of 50 - 100 Nml/min the reactor proved to behave as a plug-flow reactor with an extremely low axial dispersion (corresponding to approximately 500 "ideal mixed

tanks" (CSTR) in series).

Analysis of the gas mixture was performed with a quadrupole mass spectrometer (Balzers QMH 511) and a Carlo Erba 4200 gas chromatograph. The reactor outlet was directly connected via a fused silica capillary to the quadrupole, which enabled fast ion monitoring, controlled by a laboratory computer (typically 20 ms/amu). Within a short time a series of up to 16 samples of the product gas can be trapped in loops on a 34 port sampling valve for subsequent GC analysis. The SSTIKA experiments require that the compositions of the feed gas mixtures are identical and that there is no pressure difference between them. This was realized with electronic mass flow controllers. The pressure difference between the two gas flows was eliminated by adjusting a needle valve in the bypass.

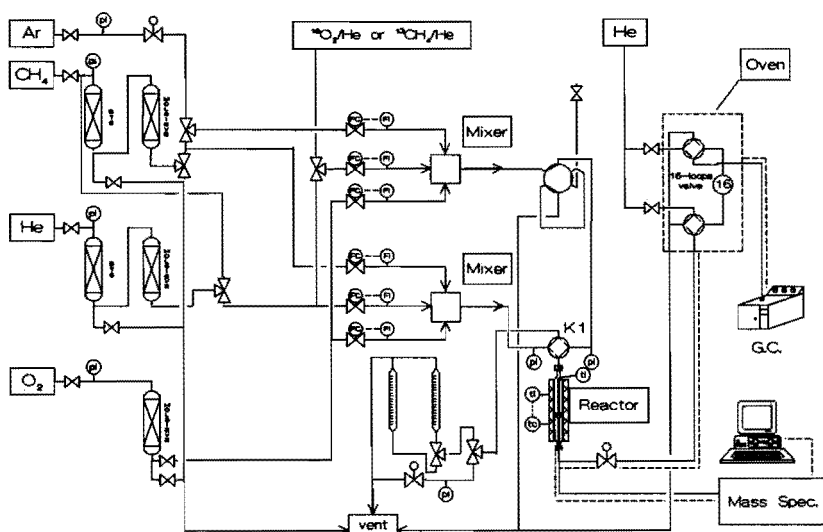


Figure 3.2.1. Reactor set-up for transient kinetic investigations.

Typical flow rates were 3.6 Nml/min methane, 9.15 Nml/min O₂/He (1:4) and 45.4 Nml/min He. The reaction temperature was 800°C and the catalyst amount 0.25 g Li/MgO. The Li/MgO catalyst used in the transient experiments was aged for 50 hours before experimentation in order to stabilize it and to eliminate the influence of catalyst deactivation.

3.3 CATALYST STABILITY

The constancy of the Li/MgO catalyst against variations in process conditions was investigated by carrying out experiments with varying process conditions. This is especially important for kinetic investigations and for the operation of the catalytic system in a commercial unit.

A series of changes in the process conditions was performed after which the standard conditions were set again to check if the performance was influenced. The standard conditions are: Temperature 800°C, $\text{CH}_4/\text{O}_2=5$, $\text{CH}_4/\text{He}=1.25$, $\text{W/F}=0.30$ g.s/ml(S.T.P.). The catalyst bed was diluted with quartz particles (50% on weight basis).

Figure 3.3.1 shows the influence of changes in process conditions on the conversion and product selectivity. The following changes were applied:

- Temperature rise to 900°C
- Feed gas composition change to helium and to oxygen/helium
- CH_4/O_2 change from 2 to 10

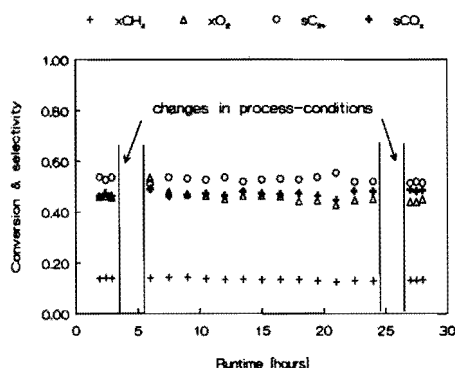


Figure 3.3.1. Methane ($x\text{CH}_4$) and oxygen ($x\text{O}_2$) conversion and product selectivities as function of time on stream with periodic disturbance of the steady state. $T=800^\circ\text{C}$, $\text{CH}_4/\text{O}_2=5$, $\text{W/F}=0.3\text{g.s/ml}$.

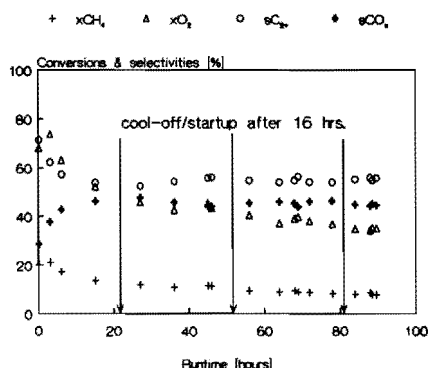


Figure 3.3.2. Methane ($x\text{CH}_4$) and oxygen ($x\text{O}_2$) conversion and product selectivities as function of time on stream with cool-off and start-up procedure. $T=800^\circ\text{C}$, $\text{CH}_4/\text{O}_2=5$, $\text{W/F}=0.3$ g.s/ml.

These changes were maintained each for 20 minutes. After one hour the standard conditions were set again and the product analysis started.

From Figure 3.3.1 it is clear that the changes in process condition do not influence the steady state operation of the catalyst. The catalyst deactivation observed is not influenced by the changes applied. In Figure 3.3.2 the influence of cool down and start up on the catalytic performance has been investigated. This means that the catalyst has been cooled down to room temperature and has been heated-up to 800°C again after

16 hours. Again no effect can be determined on the normal catalytic behaviour. It can be observed that catalyst deactivation continues even after prolonged reaction time (80 hours). Note that in Figure 3.3.2., which was started with a fresh Li/MgO catalyst, no increase in activity can be observed similar to the same experiments described in Chapter 2. In this case catalyst deactivation is occurring almost from the start of the reaction. The only difference between this experiment and the experiment in Chapter 2 (Figure 2.3.1) is the addition of quartz particles to the catalyst bed. These quartz particles are used to eliminate temperature effects. The dilution of the catalyst bed with inert particles reduces the heat production per catalyst bed volume. However, the quartz particles seem to have a dramatic effect on the catalyst stability. The deactivation of the catalyst is accelerated resulting in a rapid decline in catalytic activity.

In order to test the detrimental effect of quartz on the catalyst stability we carried out experiments with varying quartz concentration in the catalyst bed. A fixed amount of 0.4 grams of catalyst was diluted with different quantities of quartz on weight basis. These mixtures were tested under standard conditions ($W/F = 250 \text{ g.s/l}$).

Figure 3.3.3 shows the methane and oxygen conversion as a function of the reaction time for different degrees of dilution. It appears that quartz dilution has a surprisingly strong influence on the activity of the catalyst. The higher the degree of dilution the faster the catalyst deactivates. At the highest degree of dilution the catalyst deactivates already from start-up of the reaction. The maximum oxygen conversion moves to shorter reaction times as function of the degree of quartz dilution. This deactivation is most probably due to loss of lithium, which is accelerated by quartz dilution. Lithium is known to react with quartz and form lithium silicates².

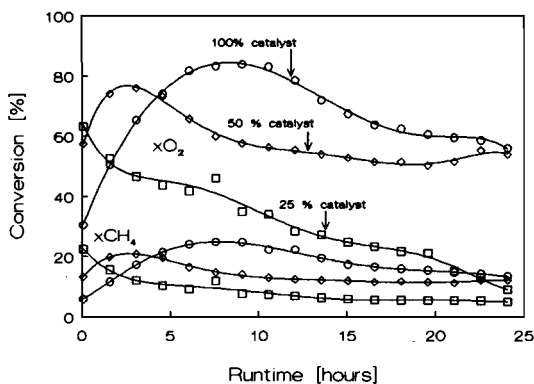


Figure 3.3.3. Methane ($x\text{CH}_4$) and oxygen ($x\text{O}_2$) conversion as function of time on stream for different quartz/Li-MgO catalyst ratios. $T = 800^\circ\text{C}$, $\text{CH}_4/\text{O}_2 = 5$, $W/F = 0.25 \text{ g.s/ml}$.

3.4 CATALYST DEACTIVATION

The Li/MgO catalyst deactivation was investigated by monitoring the lithium loss as function of the reaction time. The process conditions applied were 800°C , $\text{CH}_4/\text{O}_2 = 5$, atmospheric pressure and a 1:1 dilution with helium. Starting with a 7 wt% Li/Li+MgO catalyst a rapid loss of lithium is observed : 2 wt% in the first 15 hours (Figure 3.4.1). However, the catalytic activity is not decreasing in the first 10 hours; instead it even increases. This means that new active centres are formed and that only part of the lithium is active. It appears that only a small amount of lithium is enough to create an active and selective catalyst, as shown by experiments with a 0.2 wt% Li/Li+MgO catalyst (Figure 3.4.2).

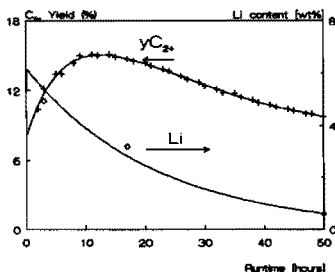


Figure 3.4.1. C_{2+} yield ($y\text{C}_{2+}$) and lithium content of a Li/MgO catalyst versus runtime. $T=800^{\circ}\text{C}$, $\text{CH}_4/\text{O}_2=5$, $W/F=0.3$ g.s/ml.

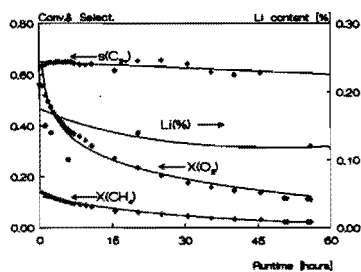


Figure 3.4.2. Methane ($x\text{CH}_4$) and oxygen ($x\text{O}_2$) conversion, C_{2+} selectivity ($s\text{C}_{2+}$) and lithium content of a Li/MgO catalyst versus runtime. $T=800^{\circ}\text{C}$, $\text{CH}_4/\text{O}_2=5$, $W/F=0.6$ g.s/ml.

In spite of the low lithium content this catalyst is reasonable active and selective. However, deactivation sets in from the start of the reaction proving that the presence of lithium is essential for the activity.

To determine the main cause of the lithium loss the lithium loss was monitored during steady state methane coupling conditions. This was compared to the lithium loss under identical conditions, but without methane in the reactor feed. Figure 3.4.3 shows the lithium content of a Li/MgO catalyst in both situations as function of time on stream. Clearly the reactant gases seem to have a much more pronounced influence on the lithium loss than an oxygen/helium mixture. The main cause for the lithium loss during steady state operation is believed to be the presence of water. Water reacts with Li_2CO_3 to CO_2 and LiOH , which is very volatile at 800°C . Korf et al³ have shown that addition of water vapour to the system indeed results in a dramatic loss of activity and lithium.

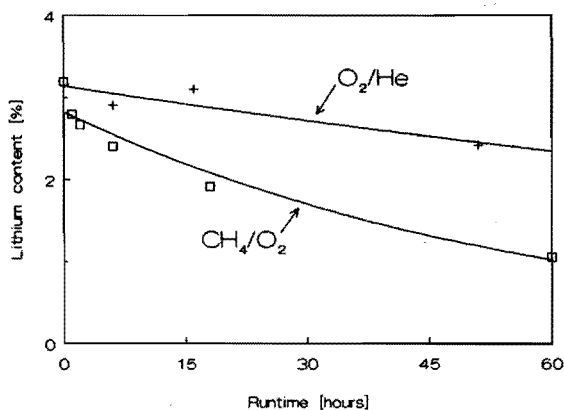


Figure 3.4.3. Lithium content of a Li/MgO catalyst as function of time on stream for a CH₄/O₂ (=5) and a O₂/He (=0.25) feed gas mixture. T=800°C, W/F=0.6 g.s/ml.

In conclusion it can be stated that the loss of lithium is mainly due to reaction of lithium with water vapour to form LiOH (volatile) and reaction with the quartz reactor wall to form catalytically rather inactive lithium silicate.

3.5 WORKING PRINCIPLE OF THE Li/MgO CATALYST

Korf et al.⁴ have shown that carbon dioxide, continuously added to the gas phase, reduces the activity of the Li/MgO catalyst, while a short treatment of a deactivated Li/MgO catalyst with carbon dioxide restores the initial activity for some time. They claim that the Li₂CO₃ phase plays an important role in the catalytic activity of Li/MgO in contrast to Driscoll et al.⁵, who stated that Li⁺O⁻ centres stabilized in the MgO matrix were the active centres for the generation of methyl radicals from methane. Especially the role of MgO is essential in Driscoll's theory, because of the substitution of Mg²⁺ ions ($r_{\text{Mg}^{2+}} = 0.66 \text{ \AA}$) in the MgO lattice by Li⁺ ions ($r_{\text{Li}^+} = 0.68 \text{ \AA}$) from the Li₂CO₃ phase.

To determine the influence of MgO on the catalytic behaviour of Li/MgO we precipitated Li₂CO₃ on another carrier material: ZrO₂. The ZrO₂ used was totally sintered so that it had only an outer surface. Because of the low surface area of the ZrO₂ particles only a small amount of lithium could be precipitated upon the particles. Figure 3.5.1 shows the activity of Li₂CO₃/ZrO₂ as function of time on stream. Clearly the oxygen conversion increases to a maximum followed by a decrease to almost no activity. Indeed the performance of this catalyst is identical to Li/MgO, except for a lower activity due to a lower surface area. The activity lasts as long as lithium is present. The interaction of ZrO₂ ($r_{\text{Zr}^{4+}} = 0.79 \text{ \AA}$) with Li₂CO₃ ($r_{\text{Li}^+} = 0.68 \text{ \AA}$) at 800°C is far less than that of Li₂CO₃ with MgO. Only at very high temperatures (>1000°C) detectable amounts of lithium zirconate (Li₂ZrO₃) are formed. It is known that ZrO₂ is capable of

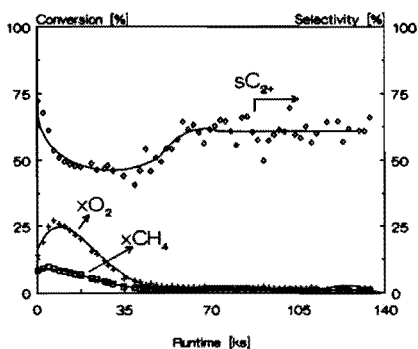


Figure 3.5.1. Methane and oxygen conversion and C_{2+} selectivity as function of time on stream for Li_2CO_3/ZrO_2 , $T=800^\circ C$, $CH_4/O_2=5$, $W/F=0.3$ g.s/ml.

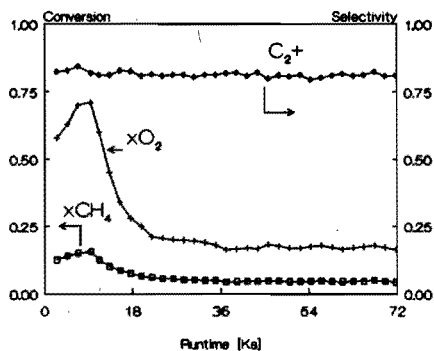


Figure 3.5.2. Methane and oxygen conversion as function of time on stream for a Li_2CO_3/Li_2ZrO_3 catalyst. $T=800^\circ C$, $CH_4/O_2=5$, $W/F=0.3$ g.s/ml.

oxygen transport in its lattice⁶. However, pure ZrO_2 as used in these experiments does not show any activity. Addition of Li_2CO_3 leads to a spectacular increase in activity at reasonable selectivity. This makes it likely that the active oxygen is formed via the lithium phase. However, it is not the lithium carbonate phase itself, which is the active phase, because experiments with pure Li_2CO_3 resulted in low C_{2+} selectivities⁷. These experiments made clear that a carrier material is needed for a selective coupling catalyst based on Li_2CO_3 . Probably the active oxygen species has to be accommodated by the carrier material as mentioned by Driscoll et al⁵.

Lithium zirconate itself appears to be a good catalyst for the oxidative coupling of methane with a reasonable activity and a high C_{2+} selectivity. Also the activity of Li_2ZrO_3 can be increased temporarily by doping it with Li_2CO_3 (Figure 3.5.2). This also indicates that very active centres for methane activation are created via the interaction of Li_2CO_3 with a carrier material like Li_2ZrO_3 . However, this catalyst also loses its activity more rapidly than Li/MgO . Due to the interaction of Li_2CO_3 with MgO the loss of the lithium phase is retarded. In that respect the MgO plays an essential role: stabilization of the lithium phase. These results clearly show that the presence of a Li_2CO_3 (precursor) phase is essential to form an active lithium catalyst. Combining of all this leads to a possible working principle of the Li/MgO catalyst shown in Figure 3.5.3. which is in agreement with Korf et al⁸.

Li_2CO_3 decomposes in the presence of oxygen to an active centre and CO_2 . This active centre reacts with methane to form a methyl radical. Deactivation of the catalyst occurs due to reaction of Li_2CO_3 with water to $LiOH$, which evaporates or Li_2CO_3 reacts with quartz to lithium silicates which are almost inert towards methane activation⁹.

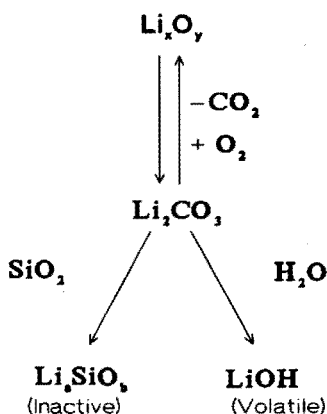


Figure 3.5.3. Working principle of the Li/MgO catalyst.

3.6 ELUCIDATION OF THE Li/MgO CATALYST WORKING PRINCIPLE BY STEADY-STATE ISOTOPIC TRANSIENT KINETIC ANALYSIS

It is not known if the Li_2CO_3 decomposition actually takes part in the formation of the active centres or in the catalytic cycle. Intriguing to know is the fact whether oxygen actually helps the decomposition of Li_2CO_3 . The use of the steady state isotopic transient kinetic analysis (SSITKA) technique, in which one labelled reactant replaces the normal species without disturbing the steady state of reaction is a way to answer this question¹⁰. We carried out experiments in which we switched from a $\text{CH}_4/^{16}\text{O}_2/\text{He}$ to a $\text{CH}_4/^{18}\text{O}_2/\text{He}$ feed gas mixture. The resulting transient curves, obtained by the continuous monitoring of the relaxation and evolution of the labelled reactants and products can be used to determine surface coverages and concentrations of active intermediates and will elucidate the oxygen pathway over Li/MgO¹¹. Analogous experiments with a switch from $^{12}\text{CH}_4/\text{O}_2/\text{He}$ to $^{13}\text{CH}_4/\text{O}_2/\text{He}$ will make it possible to determine the carbon pathway during oxidative coupling.

Figure 3.6.1 shows the oxygen response as function of the time after a switch from a $\text{CH}_4/^{16}\text{O}_2/\text{He}$ to a $\text{CH}_4/^{18}\text{O}_2/\text{He}$ feed gas mixture. Clearly it can be seen that the $^{18}\text{O}_2$ response takes at least 50 seconds before it reaches its steady state level. This means that oxygen adsorption and/or exchange with the catalyst is occurring. Also the mixed oxygen form ($^{16}\text{O}^{18}\text{O}$) is observed, which means that the $\text{O}=\text{O}$ bond is broken at the catalyst surface and that atomic oxygen is formed. During the course of the reaction the oxygen is incorporated in water and carbon dioxide. The responses of these components were also monitored by scanning the mass numbers (m/e) 20 (H_2^{18}O), 44 (C^{16}O_2), 46 ($\text{C}^{16}\text{O}^{18}\text{O}$) and 48 (C^{18}O_2). Figure 3.6.2 shows the measured response curves which result in a remarkable difference compared to the oxygen response. It takes at least 200

seconds for the $C^{18}O_2$ to reach its steady state level. This can mean for instance that slow CO_2 desorption is occurring or that slow carbonate decomposition is taking place. The latter agrees with the idea that the decomposition of Li_2CO_3 is essential in the working principle of the Li/MgO catalyst.

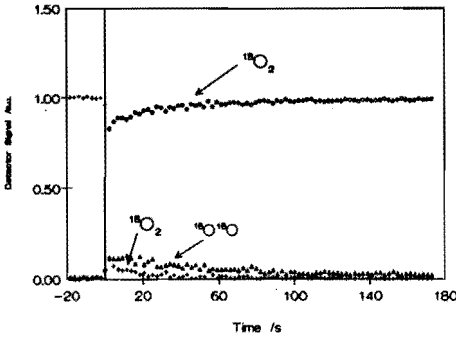


Figure 3.6.1. O_2 response after isotopic switch from $CH_4/^{16}O_2/He$ to $CH_4/^{18}O_2/He$. $T=800^\circ C$, $CH_4/O_2=1.7$, $He/CH_4=0.9$, $0.25g Li/MgO$, $W/F=0.15 g.s/ml$.

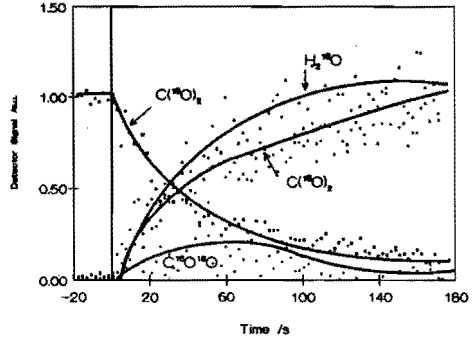


Figure 3.6.2. CO_2 and H_2O response after isotopic switch from $CH_4/^{16}O_2/He$ to $CH_4/^{18}O_2/He$. Conditions identical to figure 3.6.1.

Oxygen scrambling in CO_2 is occurring, because $C^{16}O^{18}O$ is clearly observed. The scrambling is not at the statistical equilibrium (the $C^{16}O^{18}O$ maximum should then be much higher). Peil et al¹² carried out similar isotopic switching experiments with Li/MgO , but at lower reaction temperatures, where only total oxidation reactions prevail. They found oxygen scrambling in CO_2 to be at equilibrium. In our case this is clearly not the case, probably due to the higher reaction rates at the higher reaction temperature. At these temperatures carbon dioxide is formed at a much higher reaction rate and its contact time with the catalyst surface is lowered. The water ($H_2^{18}O$) response is also very slow compared to the oxygen response, which can mean a slow water desorption from the catalyst surface or a slow rate of formation.

Table 3.6.1 shows the total rate of product formation before and after the isotopic switch confirming that no isotopic effects are occurring, which could alter the total reaction rate. Table 3.6.2 shows the total amount of ^{16}O atoms which is replaced by ^{18}O atoms. These numbers are calculated by integration of the response curves of the oxygen containing products. The sum of these numbers is the total amount of replaced ^{16}O . This number can be related to the number of atomic layers of the catalyst which take part in the oxidation process. Assuming that the catalyst contains about 10^{19} atoms/ m^2 and combining this with the surface area ($1 m^2/g$) and the catalyst amount in the reactor ($0.25g$) it can be calculated that about 10 lattice layers of a pure MgO lattice are exchanged. This means that much more than a monolayer of oxygen is taking part

in the oxidation process and thus lattice oxygen ("bulk") is participating in the oxidation process.

Table 3.6.1. Reaction rates during methane coupling over Li/MgO before and after an isotopic switch from $\text{CH}_4/^{16}\text{O}_2/\text{He}$ to $\text{CH}_4/^{18}\text{O}_2/\text{He}$. Conditions according to figure 3.6.1.

| Component | Rate/ 10^4 mole/kg cat.s. | |
|------------------------|--------------------------------|-------------------|
| | $^{16}\text{O}_2$ | $^{18}\text{O}_2$ |
| CH_4 | 10 | 10 |
| C_2H_6 | 2.8 | 2.8 |
| C_2H_4 | 0.5 | 0.5 |
| CO_2 | 3 | 4 |

Table 3.6.2. Number of exchangeable ^{16}O atoms with Li/MgO catalyst during methane coupling. $T=800^\circ\text{C}$, $\text{CH}_4/\text{O}_2=1.7$, $W/F=0.15\text{g.s/ml}$.

| Component | Number of ^{16}O 10^{19} atoms/g cat. |
|--------------------------------------|---|
| $^{16}\text{O}_2$ | 3 |
| $^{16}\text{O}^{18}\text{O}$ | 2.4 |
| C^{16}O_2 | 1.6 |
| $\text{C}^{18}\text{O}^{16}\text{O}$ | 0.25 |
| H_2^{16}O | 3.2 |
| Total | 10.5 |

The $^{13}\text{CH}_4$ switch experiments give information about the incorporation of ^{13}C into the catalyst and into the coupling products ($\text{C}_2\text{H}_6, \text{C}_2\text{H}_4$). Figure 3.6.3 shows the CH_4 response after the isotopic switch. Also a trace of argon was added to the feed to determine whether methane adsorption was occurring. As expected no measurable methane adsorption was occurring, because the methane response is identical to the argon response (not adsorbing). This effect confirms our idea that methane reacts from the gas phase with adsorbed oxygen in a ELEY-RIDEAL mechanism. Methyl radicals are released into the gas phase and couple there to form ethane. This is confirmed by the monitoring of mass (m/e) 26, which results mainly from $^{12}\text{C}_2\text{H}_4$. The $^{12}\text{C}_2\text{H}_4$ signal (not shown) appears exactly parallel to the $^{12}\text{CH}_4$ signal.

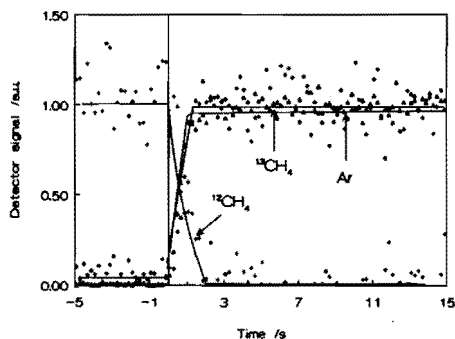


Figure 3.6.3. CH_4 response after isotopic switch from $^{12}\text{CH}_4/\text{O}_2/\text{He}$ to $^{13}\text{CH}_4/\text{O}_2/\text{He}$. $T=800^\circ\text{C}$, $\text{CH}_4/\text{O}_2=2$, 0.25 g Li/MgO , $W/F=0.25\text{ g.s/ml}$.

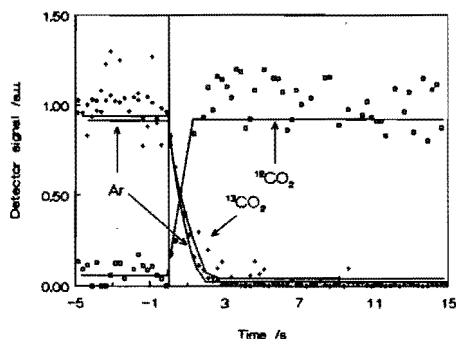


Figure 3.6.4. CO_2 response after isotopic switch from $^{13}\text{CH}_4/\text{O}_2/\text{He}$ to $^{12}\text{CH}_4/\text{O}_2/\text{He}$. $T=800^\circ\text{C}$, $\text{CH}_4/\text{O}_2=2$, $W=0.25\text{g Li/MgO}$, $W/F=0.25\text{ g.s/ml}$.

This also means that the coupling products are not adsorbed at the catalyst surface. It is further interesting to examine the carbon dioxide response, which is monitored via mass (m/e) 44 ($^{12}\text{CO}_2$) and mass 45 ($^{13}\text{CO}_2$). Figure 3.6.4 shows the CO_2 response compared to the argon trace. The responses do not differ significantly indicating that CO_2 is hardly adsorbed at 800°C . The $^{13}\text{CO}_2$ signal reaches its steady state level within a few seconds indicating that the carbon atom is not incorporated into the lattice of the catalyst to a measurable extent. This effect proves that the slow C^{18}O_2 response (200 s) shown previously, is not due to slow CO_2 desorption. The slow formation of C^{18}O_2 can be explained by assuming that carbon dioxide is mainly formed at the catalyst surface by reaction with a reactive oxygen species. This oxygen species is more reactive than the gas phase oxygen. Before C^{18}O_2 can be formed the $^{18}\text{O}_2$ must be adsorbed at the catalyst surface and the reactive oxygen species must be formed. The slow C^{18}O_2 response can so be brought back to the rate of refreshment of the active oxygen species, which is present in the Li/MgO catalyst. This phenomenon resembles the work of Van Santen and De Groot¹³, who investigated the mechanism of the ethylene epoxidation. They found that ethylene initially reacted more rapidly with preadsorbed oxygen atoms than with molecular oxygen adsorbed in the precursor state. An analogous situation seems to be the case during oxidative coupling of methane over Li/MgO.

These experiments prove that there is no large pool of a carbon containing species (like Li_2CO_3) taking part in the catalytic cycle during steady state operation. This rejects the theory of Korf et al⁷ that the active centres are involved in a continuous process of Li_2CO_3 decomposition and formation. More likely is the theory that the active centres are formed by reaction of an oxidic lithium phase, probably stabilized in the MgO matrix.

Figure 3.6.5 gives a possible oxygen pathway which explains the observed experimental results. The oxygen is adsorbed at the catalyst surface and at the same time partly incorporated into the catalyst lattice. CO_2 is formed from methane or methyl radicals colliding with the active oxygen at the catalyst surface. The CO_2 formed is not strongly bound to the surface, but released rather quickly into the gas phase. The water which is formed during the methane activation is also desorbed fast into the gas phase. This is concluded from on-off switching experiments. These experiments show that the water response is identical to the methane response. It can be concluded that more than a monolayer of oxygen is taking part in the catalytic cycle.

Figure 3.6.6 shows the working principle of the Li/MgO catalyst during oxidative coupling of methane at 800°C . Active centres are created by uptake of oxygen by the Li/MgO catalyst. These centres react with methane from the gas phase to create methyl radicals which combine in the gas phase to ethane. The Li/MgO catalyst possesses active centres which are very active in methane activation. The CO_2 , which is formed during reaction, can react with the catalyst and form extra Li_2CO_3 , although under steady state of operation this reaction hardly takes place. The lithium carbonate in turn reacts with the water, also formed during reaction and forms lithium hydroxide which evaporates

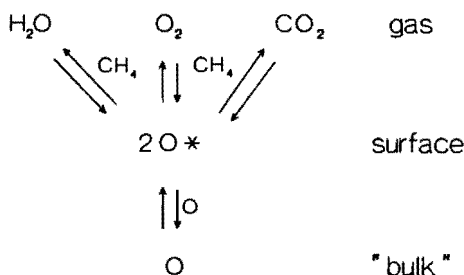


Figure 3.6.5. Oxygen pathway during methane coupling over Li/MgO.

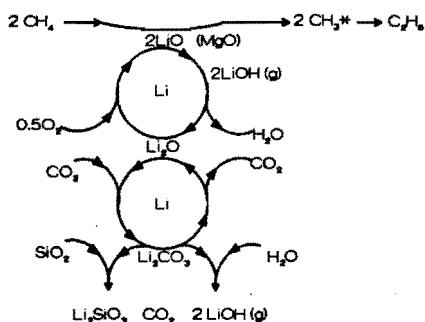


Figure 3.6.6. Working principle of Li/MgO catalyst during methane coupling.

easily at 800°C. The lithium carbonate also reacts with the quartz reactor wall and forms lithium silicates, which are inactive in methane activation. In this way the catalyst loses its lithium gradually, which in time results in deactivation of the catalyst.

3.7 CONCLUSIONS

Dilution of the catalyst bed with quartz particles increases the rate of deactivation. This is due to loss of lithium via reaction of lithium with the quartz particles under formation of lithium silicates. This silicate holds the lithium tightly so that it can no longer be of use for the formation of active centres. The more quartz is present in the catalyst bed the more this reaction will take place.

The deactivation experiments show that lithium is the active component in Li/MgO and that it is lost quite rapidly during reaction. Only a small part of the total lithium content of the catalyst is responsible for the activity. Very small amounts of lithium are sufficient to create an active and selective Li/MgO catalyst. The interaction of Li_2CO_3 with MgO is essential for the stability of the catalyst. Lithium carbonate supported on an inert carrier like sintered ZrO_2 results also in an active and selective catalyst but less stable. The excellent coupling performance of the Li/MgO catalysts is due to the formation of very reactive oxygen species which are capable of hydrogen abstraction from methane and releasing methyl radicals into the gas phase.

Experiments with the steady-state isotopic transient kinetic analysis (SSITKA) technique have shown that there exists a pool of an oxygen containing species and that there is no large pool of a carbon containing species (e.g. carbonate) in the catalyst, which is taking part in the actual catalytic cycle for methane activation. The interaction of lithium with the carrier material (MgO) causes the oxygen uptake and transport into the bulk of the catalyst. The driving force for this oxygen transport is the presence of vacancies in the MgO lattice. These vacancies are created at high reaction temperatures, especially when

the MgO is doped with lithium.

REFERENCES

1. E.E. Strange, *Anal. Chem.*, 25,4,650-651 (1953).
2. J.M.N. van Kasteren, J.W.M.H. Geerts and K. van der Wiele, *Proceedings 9th Int. Congr. Catal.*, Calgary, Canada, 2, 930 - 936 (1988).
3. S.J. Korf, J.A. Roos, N.A. de Bruijn, J.G. van Ommen and J.R.H. Ross, *Proc. EC. Congr.: "Hydrocarbons: Source of Energy"*, Eds. G. Imarisio, M. Frias and J.M. Bemtgen, Lyon, France, 441 - 450 (1988).
4. S.J. Korf, J.A. Roos, N.A. de Bruin, J.G. van Ommen, J.R.H. Ross, *J. Chem. Commun. Chem. Soc.*, 1433-1434 (1987).
5. D.J. Driscoll, W. Martir, J-X. Wang, J.H. Lunsford, *J.Am.Chem.Soc.*, 107, 58-63 (1985).
6. K. Otsuka, S. Yokoyama and A. Morikawa, *Chem. Lett.*, 319 - 322, (1985).
7. J.W.M.H. Geerts, J.M.N. van Kasteren and K. van der Wiele, *J. Chem. Soc., Chem. Commun.*, 802 -803 (1990).
8. S.J. Korf, J.A. Roos, N.A. de Bruijn, J.G. van Ommen and J.R.H. Ross, *Catal. Today.*, 2, 535 (1988).
9. J.M.N. van Kasteren, J.W.M.H. Geerts and K.van der Wiele, *Proc. 1st World Congress, New Developments in Selective Oxidation*, Eds. G. Centi & F. Trifiro, Rimini, Italy 18 - 22 september, 1989, *Stud. Surf. Sci. Catal.*, 55, 343 -352 (1990).
10. J. Happel, E. Walter and Y. Lecourtier, *Ind. Eng. Chem. Fundam.*, 25, 704-712 (1986).
11. P. Biloen, J.N. Helle, F.G.A. van den Berg, W.M.H. Sachtler, *J. Catal.* 81, 450 - 463 (1983).
12. K.P. Peil, J.G. Goodwin Jr., and G. Marcelin, *J. Phys. Chem.*, 63, 5977-5979 (1989).
13. R.A. van Santen and C.P.M. de Groot, *J. of Catal.*, 98, 530 - 539 (1986).

CHAPTER 4

ANALYSIS OF THE REACTION NETWORK

4.1 INTRODUCTION

The reaction mechanism of the oxidative coupling of methane over lithium doped magnesia comprises many elementary reactions including reactions at the catalyst surface and reactions taking place in the homogeneous gas phase.^{1 2 3 4} The reaction scheme is particularly complex, because a single reaction intermediate may be formed along various homogeneous and/or heterogeneous reaction pathways and because some reaction radicals are involved in a variety of elementary reactions.

To overcome some of the complexity problems, two special experimental methods were applied:

- 1) experiments at strongly reduced pressures and
- 2) experiments with an artificial source of methyl radicals.

The advantage of a reduced pressure is that catalytic reactions then predominate over gas phase reactions, because the chance of collision of molecules with the surface is enhanced relative to collisions between molecules in the gas phase. Moreover, consecutive reactions are strongly suppressed at low pressures, because of reduced reaction rates and hence low conversion levels. The low pressure reactor designed for these experiments was coupled to a mass spectrometer and was operated at pressures in the range of 10 - 500 Pa.

The artificial source of methyl radicals was realized in a special reactor developed in cooperation with the Physics Department of our University. It consisted of a d.c. glow discharge tube in which CH_3^* and CH_2^* radicals can be produced by interaction of argon metastables with methane. The advantage of this kind of reactor is the possibility of making a controlled amount of radicals which can be brought into contact with the catalyst. In this way a possible role of the catalyst on radical reactions can be determined.

4.2 EXPERIMENTAL

Low pressure reactor set-up

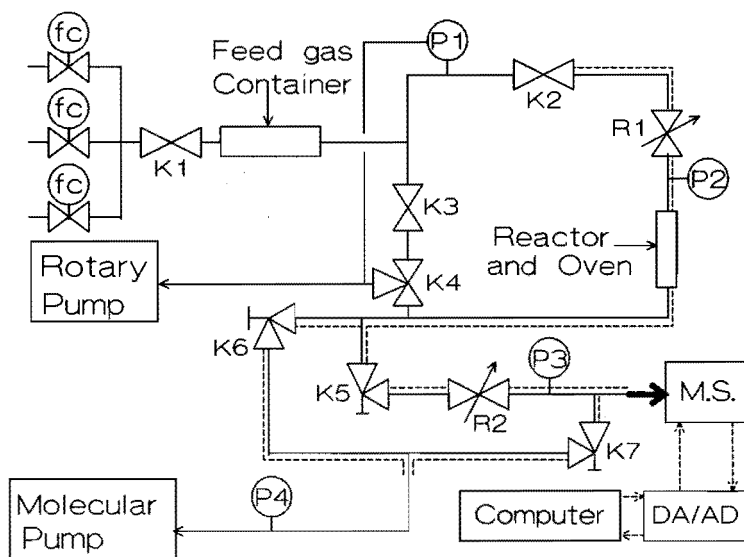


Figure 4.2.1. Reactor set-up for methane coupling experiments at low pressure. (M.S. = mass spectrometer)

The specially designed low pressure reactor set-up is shown in Figure 4.2.1. The set-up consists of a feed section with which a gas mixture can be prepared and stored in a feed gas container. From this feed gas container the gas mixture is transported to the reactor via valve K2 and leak valve R1. From there most of the gas is pumped off via three-way valve K4. Only a small amount of the product gas is used for analysis leaking via K5 and R2 to a quadrupole mass spectrometer (Leybold-Heraeus Q-200). Beside flow experiments also batch experiments were performed by closing valve K4 and K2 and leaving only the small gas leak to the mass spectrometer. The gas diffusion at these temperatures and pressures relative to the rates of reaction ($K_r \cdot d_r^2 / D_e < 0.05$; K_r is the first order reaction rate constant, d_r is the reactor diameter and D_e is the effective diffusion coefficient) assured ideally mixed conditions⁵. The reactor used is the quartz micro fixed bed reactor shown in Chapter 2.

A fresh Li/MgO catalyst was evacuated at high temperatures under low pressure conditions for 16 hours before each experiment was started. This was done to remove adsorbed gases and to stabilize the catalyst under low pressure conditions. The experiment was started by introducing the reaction gas into the reactor section. Each

process condition was maintained for 2 hours to assure stable reactivity measurements.

The analysis is performed by the Q-200 which is controlled by a computer. The concentrations of the components in the gas mixture are determined via a multiple regression program. This program uses reference spectra of the pure components to determine which ones are present (qualitative) in the gas mixture and to what extent (quantitative). The program does this by linear regression analysis between a measured mass spectrum (y_1, \dots, y_n) and a set of reference spectra (x_1, \dots, x_n). The regression has the following form:

$$\begin{array}{|c|} \hline y_1 \\ \hline y_2 \\ \hline \vdots \\ \hline y_n \\ \hline \end{array} = b_0 + b_1 * \begin{array}{|c|} \hline x_1 \\ \hline x_2 \\ \hline \vdots \\ \hline x_n \\ \hline \text{Comp.} \\ \hline 1 \end{array} + b_2 * \begin{array}{|c|} \hline x_1 \\ \hline x_2 \\ \hline \vdots \\ \hline x_n \\ \hline \text{Comp.} \\ \hline 2 \end{array} + \dots + b_p * \begin{array}{|c|} \hline x_1 \\ \hline x_2 \\ \hline \vdots \\ \hline x_n \\ \hline \text{Comp.} \\ \hline p \end{array}$$

As a result of the regression the best fitting concentration coefficients (b_0, \dots, b_p) are found, corresponding to molar fractions of the respective components. Non - significant concentration coefficients are stepwise removed in the regression procedure⁶.

Before the experiments can be carried out the quadrupole has to be calibrated. This means that the mass spectra of the expected components in the reaction mixture have to be recorded. This was done with neon as internal standard. In this way it is possible to determine a sensitivity factor for the different components. The "fingerprints" of the pure components are stored in a data file, which is used to fit the spectra of the reaction mixture⁷.

Plasma reactor set-up

The methane activation experiments were carried out in a striated column of a d.c. discharge in Ar. Figure 4.2.3 shows the reactor set-up. It consists of a feed gas section by which an argon/methane (70:1) or a CH_4/O_2 mixture can be fed to the reactor. A typical flow rate used was 18 ml/min (S.T.P.).

The reactor consists of a quartz tube ($L=60\text{cm}$, $d=2.2\text{cm}$) to which a cathode, anode and gas inlet tube are connected. The glow discharge is created by applying a 3kV voltage between cathode and anode at a reactor pressure of 3.2 mbar. The electric current is limited to 8.3 mA by means of a series resistor. The influence of the negative glow (near the cathode) with its relatively high electric field and high mean energy of the electrons is eliminated by placing the cathode in a separate chamber. The anode is shielded with a quartz tube to eliminate reactions at the anode surface. The gas inlet

position can be varied over the reactor length enabling the study of the influence of contact time. The wall of the reactor can be cooled down to liquid nitrogen temperature. In this way the reaction products are frozen at the reactor wall and a dissociation of the reaction products by metastable atoms will be prevented.

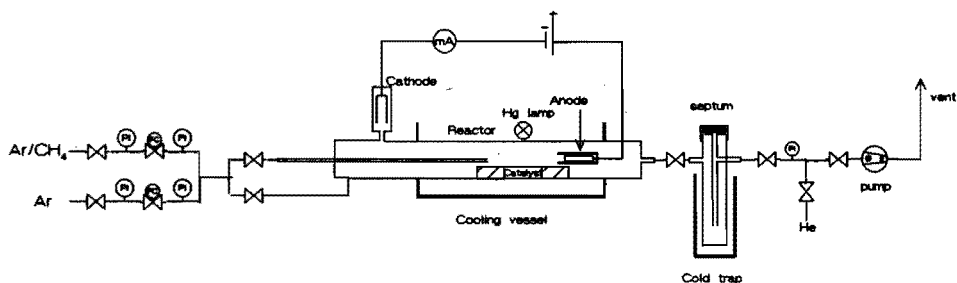


Figure 4.2.3. Reactor set-up applied for the d.c glow discharge process.

A plasma reaction was carried out by turning on the electric power for 1 minute during which the argon/methane was fed to the reactor via the variable gas inlet. The influence of catalyst surfaces on radical coupling reactions was studied by placing an amount of catalyst into the reactor filling the space between gas inlet and anode. Activation of the Li/MgO catalyst was performed by UV irradiation with a 500 W mercury vapour lamp in the presence of gas phase oxygen. The activated catalyst was exposed to the methane/argon mixture and the reaction was carried out as described above.

The products formed are collected in a cold trap (77K) and analyzed after heating to room temperature and pressurizing with helium. The analysis is performed with a Carlo Erba 4200 gas chromatograph with a flame ionization detector connected to a phenylisocyanate column to separate CH₄, C₂H₆, C₂H₄, C₂H₂, C₃H₈, C₃H₆, and C₄₊.

Lithium doped magnesia was prepared by heating a slurry of MgO (Merck p.a.) and Li₂CO₃ (Merck extra pure) in water to dryness (7 wt% Li/(Li+MgO)). The resulting paste was dried at 120°C for 16 hours and subsequently calcined 4 hours at 900°C. Finally the catalyst was ground and sieved to the desired particle size of 0.3 - 0.5 mm.

4.3 THE ROLE OF THE CATALYST IN THE METHANE COUPLING PROCESS

The role of the Li/MgO catalyst during methane coupling was investigated by continuous flow and batch experiments carried out at 50 - 150 Pa in the low pressure set-up described previously.

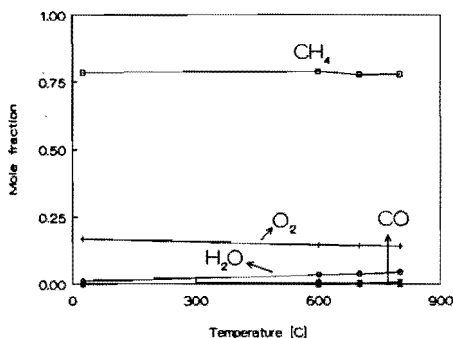


Figure 4.3.1. Catalytic methane coupling at 33 Pa over 0.25 g Li/MgO.

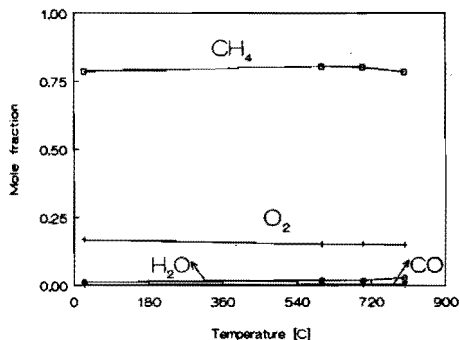


Figure 4.3.2. Gas phase oxidative coupling of methane at 33 Pa.

Figure 4.3.1 and 4.3.2 show the oxidative coupling of methane with and without a 7 wt% Li/MgO catalyst at a total pressure of 33 Pa with a gas flow rate of 10^{-7} mole/s as a function of the reaction temperature. As expected the presence of a catalyst hardly matters at the short contact times applied. At low pressure the reaction rates are lowered so longer contact times are needed to detect conversion. This can be done by carrying out batch experiments and following the course of the reaction over a long period.

Figure 4.3.3 and 4.3.4 show the methane batch oxidation with and without the presence of the Li/MgO catalyst. Again without catalyst almost no conversion can be detected during 1 hour reaction at 800°C. With catalyst clearly methane activation is occurring. Surprisingly, the C_{2+} product fraction is very low and the dominant products are the total oxidation products CO and CO_2 . This means that coupling products are not formed in a first step or that they are rapidly converted to total oxidation products at the catalyst surface. More likely however, is that at the low pressure applied the methyl radicals formed by hydrogen abstraction of methane can only react at the catalyst surface and cannot combine in the gas phase. For coupling they must lose their energy and this is (at low pressure) only possible at the catalyst surface. The chance of being oxidized at the catalyst surface is greater than coupling with another methyl radical. This theory is confirmed by atmospheric experiments with varying diluent gas concentration. Figure 4.3.5 shows the change in product selectivity as function of the helium diluent concentration during oxidative coupling of methane carried out at 100 kPa and 800°C. Clearly one can see the beneficial effect of more diluent on the C_{2+} selectivity. The partial pressures of methane and oxygen are lowered as in the low pressure experiments,

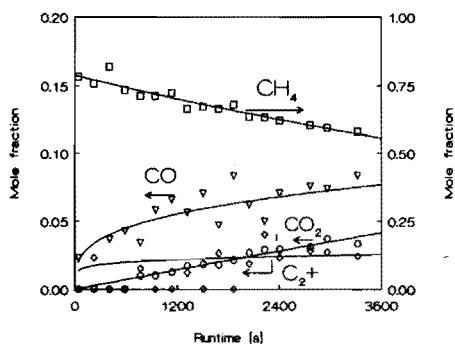


Figure 4.3.3. Methane batch oxidation over 0.25 g Li/MgO. $T=800^{\circ}\text{C}$, $P=66\text{ Pa}$.

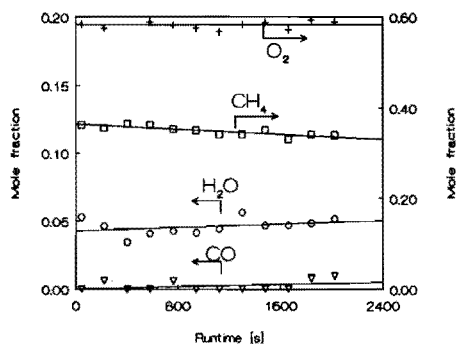


Figure 4.3.4. Methane batch oxidation without catalyst. $T=800^{\circ}\text{C}$, $P=66\text{ Pa}$.

but the total pressure remains at 100kPa. This means that gas phase coupling of methyl radicals is favoured. High concentrations of inert gas reduce the oxidation of the radicals in the gas phase and improve the radical coupling efficiency. This means that the homogeneous radical gas phase reactions play a very important part in the C₂₊ selectivity, which can be reached. This also puts constraints on the comparison of different coupling catalysts. A different diluent concentration can mean a large difference in the C₂₊ selectivity.

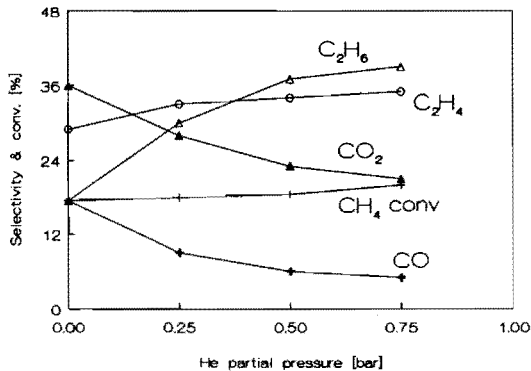


Figure 4.3.5. Methane conversion and product selectivity versus helium pressure. $T=800^{\circ}\text{C}$, $P=100\text{ kPa}$, 1g Li/MgO, $\text{CH}_4/\text{O}_2=5$, $W/F=0.6\text{ g.s/ml}$.

The reactivity of ethane and ethylene was investigated in separate experiments with a ethane/oxygen and a ethylene/oxygen feed respectively. Figure 4.3.6 and 4.3.7 show the ethane oxidation with and without catalyst as function of the temperature for a $C_2H_6/O_2/Ne$ (5/5/1) gas mixture, which was fed continuously.

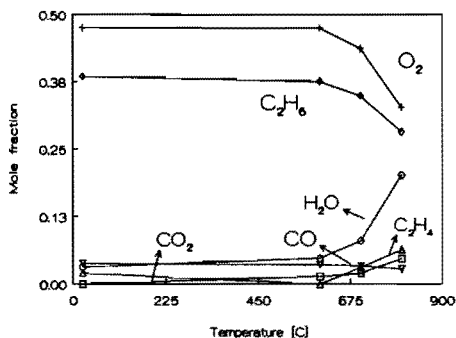


Figure 4.3.6. Ethane oxidation as function of the temperature. $P=33$ Pa, $W=0.25$ g Li/MgO, $F=10^7$ mole/s.

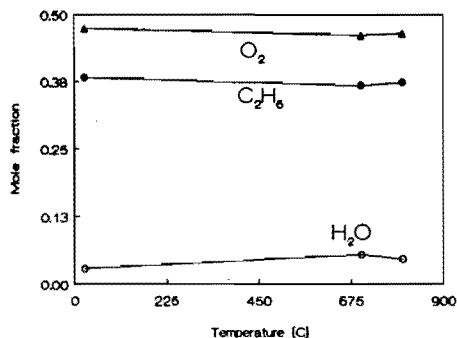


Figure 4.3.7. Ethane gas phase oxidation as function of the temperature. $P=33$ Pa, $F=10^7$ mole/s.

Gas phase oxidation does not occur, but with the Li/MgO catalyst oxidation sets in between $600^{\circ}C - 800^{\circ}C$. Beside total oxidation products ethylene is formed. It can be concluded that Li/MgO catalyses the conversion of ethane into ethylene. These experiments clearly prove that ethylene is also produced heterogeneously from ethane over Li/MgO. The same experiment carried out with an ethylene oxygen mixture showed that ethylene is catalytically oxidized to CO_x (Figure 4.3.8).

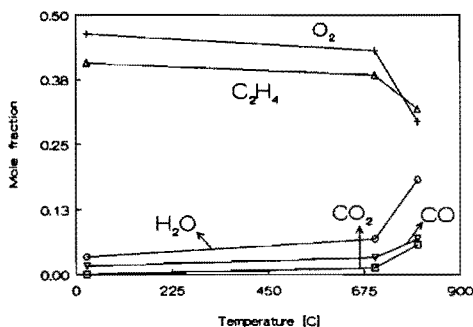


Figure 4.3.8. Ethylene oxidation over Li/MgO. $P=33$ Pa, $W=1$ g, $F=10^7$ mole/s.

It is expected that CO and CO₂ in the ethane experiment stem from oxidation of the ethylene formed⁸. The best way of showing that a consecutive reaction model is applicable in which ethane is converted to ethylene, ethylene to CO and CO to CO₂ is to carry out an ethane batch experiment.

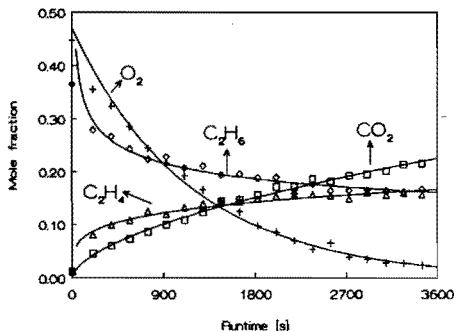


Figure 4.3.9. Ethane batch oxidation over Li/MgO at 66 Pa. $T=800^{\circ}\text{C}$, $W=0.25\text{ g}$.

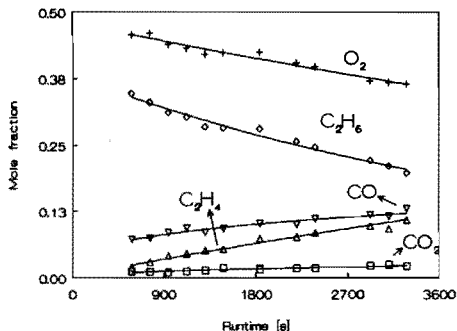


Figure 4.3.10. Ethane gas phase batch oxidation at 66 Pa. $T=800^{\circ}\text{C}$.

Figure 4.3.9 shows the product distribution of an ethane oxygen batch experiment over Li/MgO. Clearly the fraction of ethylene is coming up first followed by CO₂. CO is hardly occurring indicating that CO is relatively rapid converted to CO₂. This last reaction is definitely catalyzed by the Li/MgO catalyst, because the same experiment without catalyst shows that CO and C₂H₄ are the main products (Figure 4.3.10). This gas phase batch experiment shows that the consecutive reaction network is also valid in the gas phase, but that this takes place at a much slower rate than the heterogeneous oxidations.

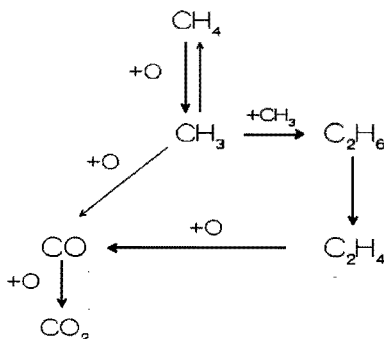


Figure 4.3.11. Reaction network of the methane coupling over Li/MgO

The reaction network of the methane coupling over Li/MgO can be summarized as shown in Figure 4.3.11. Methane is converted at the catalyst surface to methyl radicals which couple in the gas phase to ethane. At the same time the methyl radicals can be oxidized heterogeneously to CO_x . The ethane dehydrogenation and the subsequent oxidation of the ethylene formed can take place both in the gas phase and on the catalyst in heterogeneous reaction steps. The conversion of the CO to CO_2 is definitely a fast heterogeneous process.

4.4 THE ROLE OF THE CATALYST IN CONSECUTIVE REACTIONS

As described in paragraph 4.3 the main reaction path for the formation of ethylene in the oxidative coupling of methane over Li/MgO catalysts is a consecutive path in which methane is catalytically activated to form methyl radicals which combine to ethane, followed by dehydrogenation of ethane to ethylene. It is often assumed that homogeneous reactions predominate at 800°C , apart from the initial methyl radical formation. However, the catalyst may play an important role as well, particular in activation of ethane and ethylene to take part in consecutive reactions. Comparison between the reactivity of methane, ethane and ethylene over Li/MgO can be achieved with the aid of admixing experiments at low pressure. Therefore experiments with $\text{CH}_4/\text{C}_2\text{H}_6/\text{O}_2$ and $\text{CH}_4/\text{C}_2\text{H}_4/\text{O}_2$ mixtures were carried out in the special micro-flow reactor operating at low pressures (10-150 Pa) as described in paragraph 4.2.

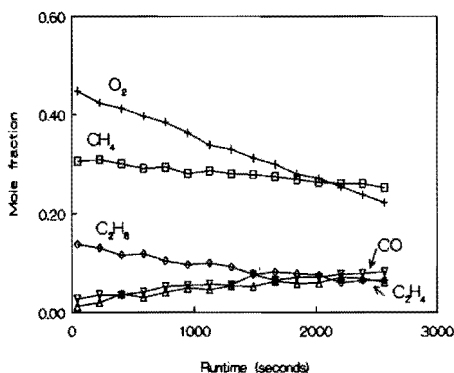


Figure 4.4.1. $\text{CH}_4/\text{C}_2\text{H}_6/\text{O}_2$ admixing batch experiment at 66 Pa. $T=800^\circ\text{C}$, $W=0.25\text{g Li/MgO}$.

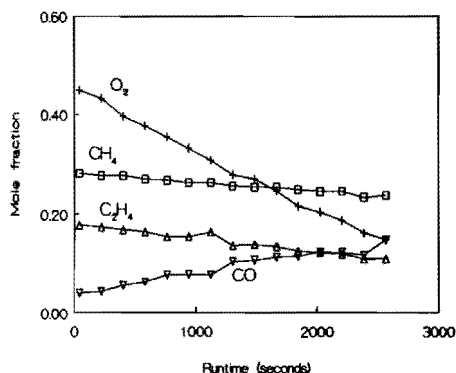


Figure 4.4.2. $\text{CH}_4/\text{C}_2\text{H}_4/\text{O}_2$ admixing batch experiment at 66 Pa. $T=800^\circ\text{C}$, 0.25g Li/MgO .

Figure 4.4.1 and 4.4.2 show $\text{CH}_4/\text{C}_2\text{H}_6/\text{O}_2$ and $\text{CH}_4/\text{C}_2\text{H}_4/\text{O}_2$ admixing experiments carried out in the batch mode of operation at 66 Pa in the low pressure reactor set-up. The results confirm that ethane and ethylene are activated more easily than methane, in agreement with experiments with the separate components⁹. The reacting ratios can be quantified by calculating rate coefficients from the data in Figures 4.4.1 and 4.4.2. For these calculations very simple power law rate equations are applied in which a reaction order of 1 is assumed for both the hydrocarbon and the oxygen. The rate equation has the following form:

$$r_i = k_i \cdot p_i \cdot p_{\text{O}_2}$$

in which i stands for CH_4 , C_2H_6 or C_2H_4 . As stated in Chapter 3 Eley - Rideal type of equations are more appropriate, but at these low pressures they degenerate anyhow to the simple form used here. When using the simple power law equations, it is assumed that methane, ethane and ethylene oxidation rates are not influenced by each other otherwise than competing for the same active oxygen on the catalyst. The amount of C_2 formed from methane in the experiments depicted in Figure 4.4.1 and 4.4.2 can be assumed negligible and is not accounted for. Table 4.4.1 shows the results of the calculations.

Table 4.4.1. k values (mole/kg cal.s.(bar)²) based on power law rate equations. Consecutive model applied to methane oxidation over 0.25 g Li/MgO at 66 Pa and 800°C.

| k_{CH_4} | $k_{\text{C}_2\text{H}_6}$ | $k_{\text{C}_2\text{H}_4}$ | $k_{\text{C}_2\text{H}_6}/k_{\text{CH}_4}$ | $k_{\text{C}_2\text{H}_4}/k_{\text{CH}_4}$ |
|-------------------|----------------------------|----------------------------|--|--|
| 0.16 | 0.64 | 0.42 | 4 | 2.6 |

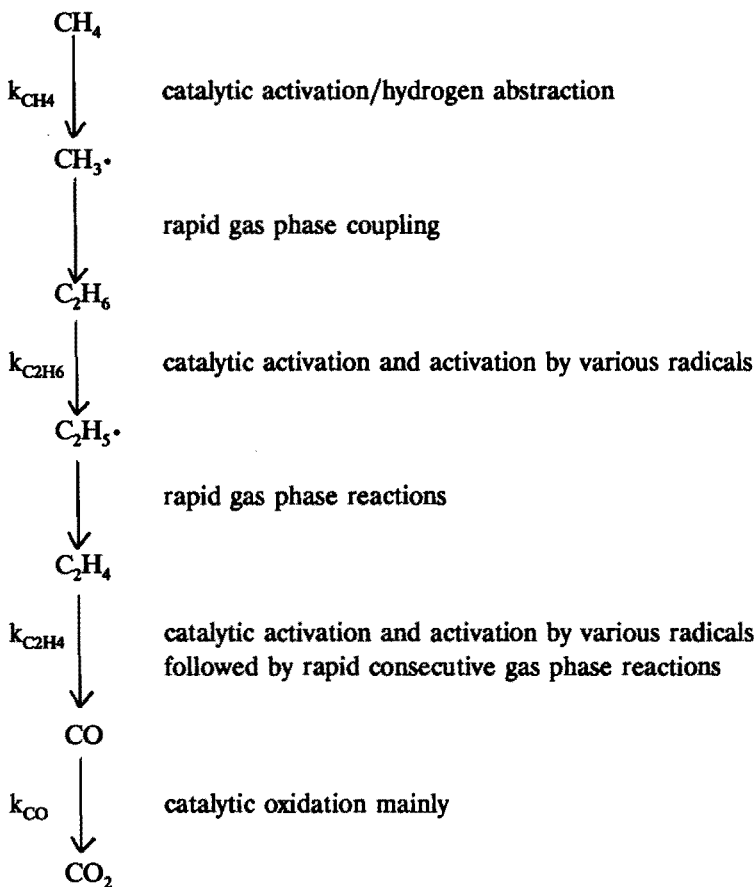
Comparison of these k -values clearly shows that ethane and ethylene are activated at least a factor 2 easier than methane. This is in agreement with the higher stability of the methane molecule compared to the C_{2+} hydrocarbons.

The results make also clear that ethane is converted a factor 1.5 faster than ethylene. This is in agreement with the results of admixing experiments carried out at atmospheric pressure¹⁰, although the difference is much more pronounced in that case: at atmospheric pressure it hardly makes any difference whether ethane or ethylene is fed together with methane and oxygen: the product distribution is practically the same. Apparently there is a particularly large contribution of gas phase reactions in the ethane to ethylene conversion.

The relatively high rate of ethylene oxidation with respect to the methane conversion restricts the C_2 yield that can be reached with Li/MgO to a maximum. In fact, the factor 2.6 for the ethylene oxidation is a lower limit based on catalytic reactions alone. At atmospheric pressure this factor is substantially higher due to the contribution of gas

phase reactions, as will be shown below, and accordingly the attainable yields are then lower.

The results presented here confirm the reaction scheme for the methane oxidative coupling (at 1 bar and 800°C) as proposed earlier⁸:



The direct oxidation of $\text{CH}_3\cdot$ to CO/CO_2 is omitted although it does occur both as a catalytic reaction (as shown above) and as a gas phase reaction; however, using Li/MgO at favourable conditions, the reaction is of minor interest.

Based on this simplified reaction scheme, a mathematical model was set up to describe the reaction and to predict maximum attainable C_2 yields. The rate equations are based on the power law equations described previously. Thus the hydrocarbons are assumed to react according to the k -ratios calculated from the low pressure experiments (Table 4.4.1).

Figure 4.4.3 shows the C_{2+} yield as function of the contact time for different CH_4/O_2 ratios. Dependent on this ratio the highest C_{2+} yield to be reached lies around 35%. This excellent value is enough for an economically attractive process¹¹. In practice however, it is not possible to eliminate the non selective gas phase reactions which will lower the C_{2+} yield⁴. The practical C_{2+} yield will always be lower than the theoretical yield, but it should be possible to reach the target value of 25%.

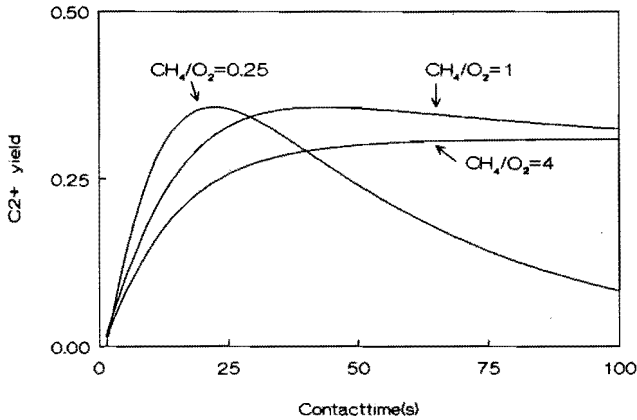


Figure 4.4.3. C_{2+} yield as function of the contact time for different CH_4/O_2 ratios as result from model calculations based on a consecutive model for methane coupling.

4.5 INTERACTION OF RADICALS WITH Li/MgO

Radical reactions play a very important role in the oxidative coupling of methane over Li/MgO catalysts. To investigate the influence of the catalyst on recombination reactions the dissociation of methane by the catalyst is replaced by producing radicals in a special way: by passing methane through a tube in which a striated column of a d.c. glow discharge in argon is generated. This technique offers the unique advantage of the sole production of CH_3 and CH_2 radicals without total destruction of the methane molecule. These radicals can be brought into contact with a catalyst present in the reactor. With this technique the influence of high temperatures is eliminated and the amount of radicals produced can be controlled.

Various types of discharges exist dependent on the gas pressure and the voltage applied. Figure 4.5.1 shows a classification of discharges by means of voltage and electric current applied¹². The discharge, which has been used in this investigation, is the normal glow discharge. It was operated at about 3kV and 7 mA.

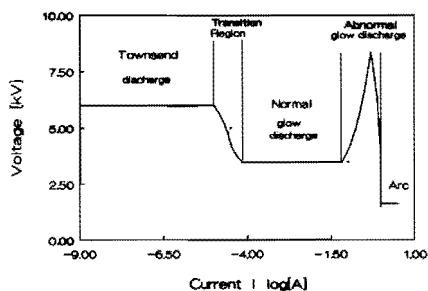


Figure 4.5.1. D.C. discharge classification

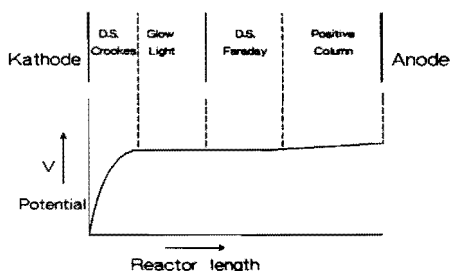


Figure 4.5.2. Evolution of the potential for a d.c. glow discharge. (D.S. = dark space).

The normal glow discharge consists of zones with different properties. Figure 4.5.2 shows the potential versus the distance between the cathode and anode. As can be seen the potential difference is large close to the cathode, whereas in the positive column hardly any potential difference exists. The positive column contains so called striae: light layers in which electrons are accelerated to the excitation energy of the main gas. In the positive column the concentration of high energy electrons is limited (and thus their influence), because these electrons possess their high energy only for a very short time. The high energy electrons are only created in the active part of the striae which is an electric double layer. As such a layer is very narrow it assures that the electrons are accelerated almost without collisions. After passage of the electrons through this layer collisions and excitation take place, resulting in Ar metastables. The remaining energy

of the electrons is small with respect to the energy of the excitation levels of interest. The formation of Ar ions in an interaction of an electron with a metastable is negligible. Therefore, only one source of energy is present in the positive or striated column of Ar which we apply: a relatively high concentration of metastable atoms.¹³ These argon metastables are the main energy source which causes the dissociation of the methane molecules in the striated column. The concentration of the metastable atoms may be calculated from the decay frequencies of several long living particles as measured and discussed by A.V. Phelps.¹⁴ In our case the concentration of Ar metastables lies around 0.1% of the gas molecules present at 3.2 mBar.¹⁵

The Ar metastable atom is used to activate methane. The energy of the metastable atom is 11.5eV being too low to enable ionization of methane (12.6eV). Dissociation of one or two H atoms from methane is the main reaction resulting in CH_3 and CH_2 radicals.

Low pressure conditions in connection with a cooled wall (77K) assure that the radical reactions mainly take place at the reactor wall. This is due to the fact that the coupling of two radicals requires a third body to compensate for the kinetic energy and mechanical impulse, provided that no chemiluminescence occurs, as is the case.

Figure 4.5.3 shows the product distribution of typical methane activation experiments at two reactor wall temperatures: 293 K and 77 K. Ethane and acetylene are the main products formed while minor amounts of ethylene, propylene, propane and butane were detected.

Apparently ethane results from the coupling of methyl radicals. Acetylene assumably stems from the reaction of CH_2 radicals under emission of hydrogen atoms or molecules.

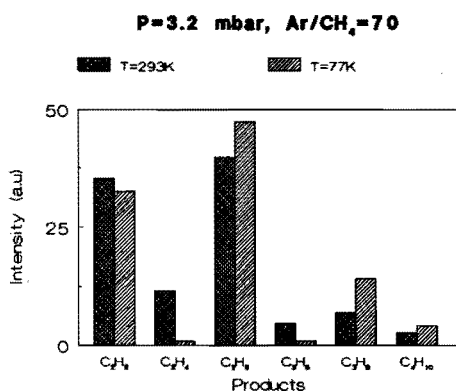


Figure 4.5.3. Product distribution of light hydrocarbons formed during methane activation in the striated column discharge.

Ethylene (and propylene) are clearly originating from consecutive reactions, e.g. the attack of metastables on ethane and propane. This is proven by the fact that at 77 K alkenes are hardly formed, because the primary products then stick to the wall. Consecutive reactions result not only in dehydrogenation, but also in the formation of higher hydrocarbons, as shown in Figures 4.5.4 and 4.5.5, which depict experiments in which the position of the gas inlet tube and hence the reaction time is varied.

Figure 4.5.4 demonstrates that the methane conversion increases with reaction time, but that most of the methane is converted into higher hydrocarbons ($>C_{2.4}$), which remain adsorbed at the tube wall at room temperature. This was also confirmed by performing a long time experiment. After a few hours a dark coloured deposit on the reactor wall can be seen. The same experiment at 77K resulted in a light coloured deposit on the reactor wall, which indicates that no elementary carbon was formed. Figure 4.5.5 shows the product distribution of the light hydrocarbons as function of the position of the gas inlet tube. The amount of ethane decreases at longer contact times at the expense of the formation of higher hydrocarbons ($>C_2$). This clearly demonstrates the involvement of ethane in consecutive reactions.

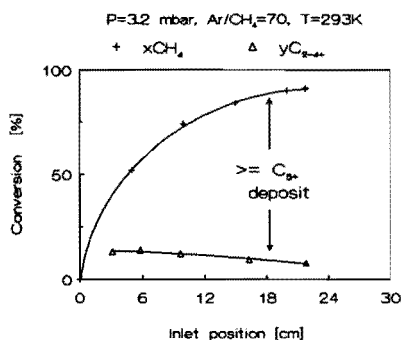


Figure 4.5.4. Overall methane conversion and methane conversion to C_{2-4} hydrocarbons.

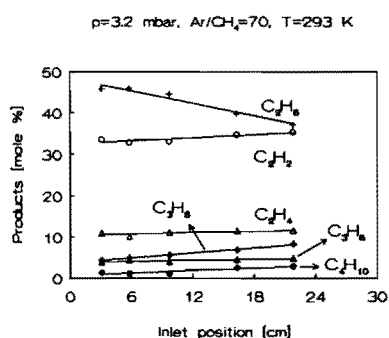


Figure 4.5.5. Product distribution of light hydrocarbons versus the gas inlet position.

The occurrence of a waxy deposit on the reactor wall implies the occurrence of a radical chain growth reaction mechanism. Such a mechanism can be described by a reaction model as applicable in the Fischer - Tropsch synthesis¹⁶. Figure 4.5.6 shows the possible reaction mechanism for the chain growth propagation mechanism applicable for the striated column synthesis. If the chance of chain growth propagation (reaction with a $CH_2\cdot$) is (a) and that of termination (reaction with a $CH_3\cdot$ radical) is (1 - a) and independent from the chain length, the mole fraction of the products formed (F_{mol}) can be determined according to the formula:

$$F_{mol} = a^{n-2} * (1-a)$$

a = rate of chain growth propagation/total rate

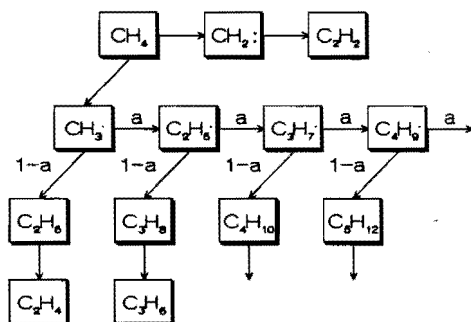


Figure 4.5.6. Reaction scheme of methane activation in a striated column of an Ar glow discharge.

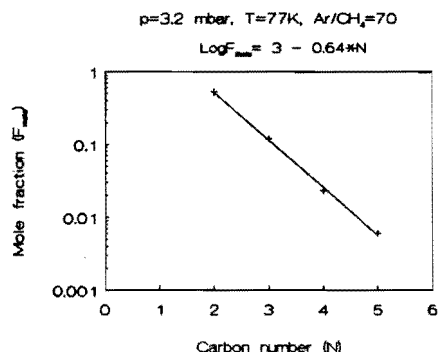


Figure 4.5.7. The product mole fraction versus the carbon number.

From the slope of the line in Figure 4.5.7, which shows the logarithmic plot of the mole fraction of the products formed versus the carbon number, it can be deduced that the $a = 0.24$. In this plot the F_2 mole fraction does not contain C_2H_2 , because the latter is assumed to be made via the coupling of two CH_2 radicals. A slope of 0.24 means that mainly short (light) hydrocarbons are formed. In the absence of oxygen chain growth takes place resulting in long hydrocarbons ($> C_{5+}$). During oxidative coupling of methane long hydrocarbons cannot be formed, because they are mainly oxidized to CO_x .

The oxidative conversion of methane to higher hydrocarbons using a catalyst is also believed to proceed via a radical reaction mechanism. The function of the Li/MgO catalyst is to activate methane and form radicals which react further in the gas phase. Placing the Li/MgO catalyst in the plasma reactor may reveal a possible role in radical coupling reactions. According to Ito et al.² Li^+O^- centres are the main source for methane activation. These centres are formed at high temperatures in the presence of gas phase oxygen. The same centres can also be formed at 100K by UV irradiation.

Figure 4.5.8 shows the EPR spectra of a Li/MgO catalyst in liquid nitrogen irradiated with a mercury vapour lamp or quenched from 1073 K. At a $g=2.054$ clearly a peak can be seen which can be ascribed to Li^+O^- centres stabilized in the MgO matrix¹⁷. The other peaks are due to the impurities Fe^{3+} , Cr^{3+} , Mn^{2+} and Cu^{2+} in the catalyst¹⁸.

With the aid of UV irradiation at 77K it is possible to test if methane activation is possible by Li^+O^- centres at these low temperatures. This test is performed by irradiating the Li/MgO catalyst in situ at 77K and 1 bar in the presence of methane and oxygen for 30 minutes. No coupling products were detected after heating to room temperature indicating that no significant methane activation had occurred. This seems in contradiction with Aika et al.¹⁹ who claim methane activation at room temperature on MgO. However, they used N_2O as reactant to create O^- on large surface area MgO, which does not result in the same active centres (Li^+O^-) created on Li/MgO by

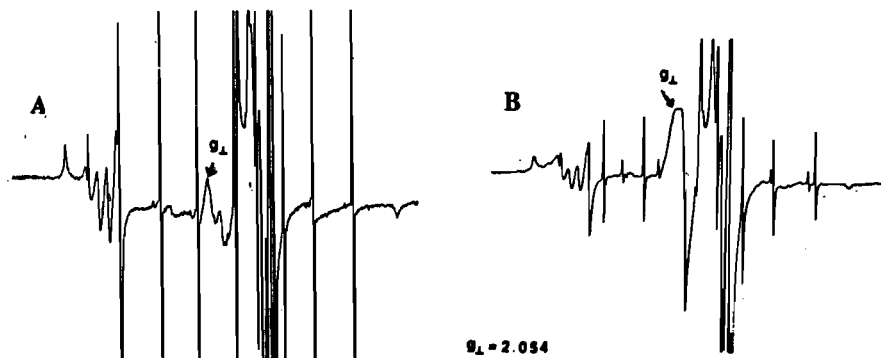


Figure 4.5.8. EPR spectra of Li/MgO catalyst quenched (A) in liquid nitrogen after heating in oxygen at 800°C or irradiated at 100K (B).

irradiation in the presence of gas phase oxygen. They detected products from methane activation only after applying very long contact times (>2 hours) and after heating the catalyst to 300°C. Further it is known that methane activation is the most difficult step in the oxidative coupling of methane²⁰. So at low temperatures it is expected that methane activation would be very difficult in contrast to Aika's results. Ceyer et al.²¹ have shown from molecular beam experiments that methane activation occurs only when the methane molecule has enough kinetic energy to deform when colliding with the catalyst surface. The deformation of the methane molecule ends the shielding of the carbon atom by the hydrogen atoms and makes surface interaction with the carbon atom possible. However, even at low temperatures there is always a small fraction of methane molecules, which has this large energy content. In Aika's experiments it cannot be excluded that the low temperature activation of methane molecules is due to that small fraction of methane molecules, which has an energy high enough to be activated at collision with the catalyst surface. A gas with a temperature of 77 K still contains 4% of molecules with a temperature velocity of 473K, assuming Maxwell velocity distribution.

Table 4.5.1. Product distribution (mole %) of plasma reaction with and without Li/MgO catalyst. $T=77K$, $Ar/CH_4=70$, $P=3.2$ mbar.

| Wall | C_2H_6 | C_2H_4 | C_2H_2 | C_3H_8 | C_3H_6 | C_4H_{10} |
|----------|----------|----------|----------|----------|----------|-------------|
| Li/MgO | 45 | 5 | 41 | 5 | 1 | 3 |
| Li/MgO* | 43 | 3 | 42 | 7 | 1 | 4 |
| Quartz | 46 | 1 | 33 | 14 | 2 | 4 |
| Quartz** | 44 | 11 | 33 | 6 | 4 | 2 |

*) UV irradiated Li/MgO.

**) $T=293$ K.

This means that methane activation with O^- is not so easy as Aika claims.

The effect of the Li/MgO catalyst on radical coupling reactions is investigated by carrying out methane activation experiments with the striated column in the presence of activated Li/MgO. Table 4.5.1 shows the product distribution of a plasma activation experiment with and without activated Li/MgO in the reactor.

There are differences in product distribution which can be ascribed to the presence of Li/MgO in the reactor. The catalyst produces more acetylene at the expense of propane, implying that the chain growth is retarded. This means that the catalyst favours the coupling of CH_2 radicals provided that the assumption that C_2H_2 is formed by coupling of two CH_2 radicals is correct. However, no difference was detected between activated and non activated Li/MgO. Probably the number of active sites is too low to detect any significant difference. Therefore no conclusion can be drawn concerning the role of Li^+O^- centres in radical coupling reactions. It is clear, though, that the nature of the catalyst surface can have an effect on the radical reactions occurring.

4.6 CONCLUSIONS

Low pressure experiments give substantial information on the reaction mechanism of the catalytic oxidative coupling of methane. It makes discrimination between homogeneous and heterogeneous reactions possible. The role of the Li/MgO catalyst during oxidative coupling of methane is that of a methane activator which produces methyl radicals which couple preferentially in the gas phase. The ethane and ethylene formed are rapidly oxidized to CO and CO_2 at the catalyst surface. A high diluent concentration in the gas phase strongly influences the C_{2+} selectivity by favouring the coupling of methyl radicals in the gas phase and thus preventing their oxidation.

The importance of consecutive reactions in the oxidative coupling of methane over Li/MgO catalysts has been demonstrated by admixing experiments carried out at low pressures (10 - 100 Pa). The relative reactivities for methane, ethane and ethylene activation by Li/MgO have been determined. Ethane is clearly the least stable. It is converted 4 times faster than methane, primarily to ethylene. Ethylene in turn is oxidized a factor 2.6 faster than methane.

The maximum achievable C_{2+} yield can be calculated by using the relative reactivities in a consecutive reaction model. The highest theoretically achievable C_{2+} yield lies around 35%. In practice, however, this value is considerably lower, because of the occurrence of non selective gas phase reactions. Further optimization of the interaction of the homogeneous and heterogeneous reactions is the way to achieve high C_{2+} yields.

A striated column of d.c. glow discharge in argon makes it possible to activate methane and produce CH_3 and CH_2 radicals. Ionization and dissociation of more than two hydrogen atoms do not occur as primary process.

Beside C_2H_6 , C_2H_2 is formed as primary product indicating that it is formed primarily

via coupling of two CH_2 radicals. The product formation in the striated column can be described by the Fischer - Tropsch chain growth propagation mechanism.

A cold Li/MgO wall obtained by covering the glow discharge tube with a thin layer of catalyst on the inside, has little influence on the recombination reactions taking place, except for an inhibiting effect on the chain growth propagation. Activation of the Li/MgO catalyst by UV irradiation in the presence of gas phase oxygen prior to the methane activation experiments does not influence the product distribution probably due to the low concentration of the active centres (Li^+O^-) formed.

Activation of methane with Li^+O^- centres created at low temperatures with aid of UV irradiation to give C_{2+} hydrocarbons without discharge appeared impossible.

REFERENCES

1. D.J. Driscoll, W. Martir, J-X Wang and J.H. Lunsford, *J. Am. Chem. Soc.*, 107, 58-63 (1985).
2. T. Ito, J-X Wang, C.H. Lin and J.H. Lunsford, *J. Am. Chem. Soc.*, 107, 5062-5068 (1985).
3. C.A. Jones, J.J. Leonard and J.A. Sofranko, *J. Cat.* 103, 311 (1987).
4. J.M.N. van Kasteren, J.W.M.H. Geerts and K. van der Wiele, *Proc. 9th Int. Congr. Catal.*, Calgary, Canada, 2, 930-936 (1988).
5. L.B.B.M. Janssen, M.M.C.G. Warmoeskerken, *Transport Phenomena Data Companion*, Delftse Uitgevers Maatschappij B.V. (1987).
6. D.D. Tunnicliff and P.A. Wadsworth, *Anal. Chem.*, 37 (9), 1082 - 1085 (1965).
7. A.J. van de Beek, Master Thesis, University of Technology Eindhoven, The Netherlands (1989).
8. J.W.M.H. Geerts, PhD Thesis University of Technology Eindhoven, The Netherlands (1990).
9. J.M.N. van Kasteren, J.W.M.H. Geerts and K. van der Wiele, *Catal. Today*, 6, 497 - 502 (1990).
10. J.W.M.H. Geerts, J.M.N. van Kasteren and K. van der Wiele, *Proceedings EC Congr.: 'Hydrocarbons: Source of Energy'*, Eds. G. Imarisio, M. Frias and J.M. Bemtgen, Lyon, France, 434 - 440 (1988).
11. J.W.M.H. Geerts, J.M.N. van Kasteren and K. van der Wiele, *EC contract EN3C-0038-NL (GDF), Final Report (1990)*.
12. F.M. Penning, *Elektrische gasontladingen*, Servire, Den Haag (1955).
13. J.G.A. Hölscher, *Proceedings 8th Int. Conf. on Chem. in Ionized Gases*, Vienna, 108 (1967).
14. A.V. Phelps, *Phys. Rev.*, 99, 1307 (1955).
15. A.H. Futch and F.A. Grant, *Phys. Rev.*, 104 (2), 356 - 361 (1956).
16. P. Biloen, W.M.H. Sachtler, *'Advances in Catalysis'*, Academic Press, London, 30, 165 - 214 (1981).
17. J-X. Wang and J.H. Lunsford, *J. Phys. Chem.*, 90, 5883 - 5887 (1986).
18. Y. Chen, H.T. Tohver, J. Narayan and M.M. Abraham, *Phys. Rev. B*, 16 (12), 5535 - 5542 (1977).
19. K. Aika and J.H. Lunsford, *J. Phys. Chem.* 81 (14), 1393 - 1398 (1977).
20. N.W. Cant, C.A. Lukey, P.F. Nelson and R.J. Tyler, *J. Chem. Soc., Chem. Commun.*, 766 - 767 (1988).
21. S.T. Ceyer, Q.Y. Yang, M.B. Lee, J.D. Beckerle and A.D. Johnson, *Methane Conversion*, Eds. D.M. Bibby, C.D. Chang, R.F. Howe and S. Yurchak, 51 - 66 (1988).

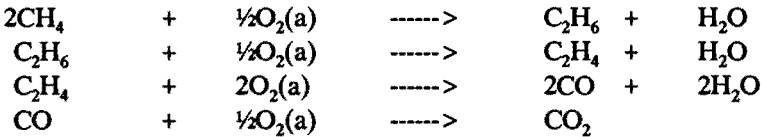
CHAPTER 5

KINETIC MODELLING

5.1 INTRODUCTION

The experiments described in Chapter 4 resulted in kinetic data for the essential heterogeneous reaction steps, which occur during oxidative coupling of methane over Li/MgO. The homogeneous reaction steps (gas phase) however, play an important role in the reaction mechanism, as the ethane formation mainly takes place in the gas phase by methyl radical coupling. Therefore kinetic measurements at realistic process conditions are indispensable. Moreover, the kinetic parameters are needed for the reactor design and process development.

Any kinetic modelling is always based on an assumed reaction mechanism. The reaction mechanism used in this chapter is based on the results from Chapter 3 and 4. Methane reacts with adsorbed oxygen on the catalyst according to an Eley - Rideal mechanism. As a result methyl radicals are released into the gas phase where ethane formation takes place by radical coupling reactions. The ethylene is formed by dehydrogenation of the ethane formed. CO and CO₂ are mainly a result of the oxidation of ethylene. The overall equations are:



The reaction mechanism is extensively being discussed in literature. Korf et al.¹ propose a Langmuir - Hinshelwood type of mechanism as the best fit for their kinetic measurements. Methane, oxygen and carbon dioxide are competing for the same adsorption site, the reaction of adsorbed methane and oxygen being the rate determining step. The transient experiments (Chapter 3) have shown that methane adsorption is very weak at 800°C especially compared to the oxygen adsorption. Therefore an Eley -Rideal mechanism appears much more realistic.

In this chapter differential kinetic measurements are described, carried out in a micro flow reactor at atmospheric pressure. To assure correct kinetic measurements we first carried out some experiments to check the absence of mass transfer limitations, which might disturb the kinetic analysis.

5.2 EXPERIMENTAL

The differential kinetic experiments were carried out in the continuous oxidation set-up described in Chapter 2.

The process conditions applied were : temperature 800°C, pressure 1 bar, total flow rate = 8.33 Nml/s, catalyst weight = 0.25 g. The fresh catalyst contained 4.27% Li/(Li+MgO) and the particle size used was 0.25 - 0.30 mm.

The reaction rate was measured after the rate of deactivation of the catalyst had been decreased to an acceptable level (approximately after 40 hours on stream). The reaction rate was measured for four different methane and oxygen concentrations in the feed gas mixture. The reaction rate (r_m) was calculated as mole/kg cat. s. :

$$r_m = F_m/W * X_m$$

W = Catalyst weight (kg)

F_m = Flow rate in mole CH_4 /s

X_m = Methane conversion

The catalyst deactivation continues even after prolonged reaction time. It is therefore necessary to carry out kinetic measurements within the shortest possible time range. The most accurate experiments were carried out within the time range of a few hours. Even then repeated experiments at standard conditions were required to measure deactivation and to account for it in the interpretation of the results.

5.3 MASS TRANSFER LIMITATIONS

Mass transfer limitations regarding solid catalysts are divided into two areas: internal and external.

Internal diffusion limitation is related to the pore structure of the catalyst. The catalyst particle size determines the pore length over which the gaseous reactants have to diffuse. The time that the reactants remain in the pores in relation to their reactivity is a measure for the occurrence of internal diffusion limitations. These limitations can have effects on the product selectivity. The occurrence of internal transport limitations was investigated by carrying out catalytic experiments with varying catalyst particle size (0.1 to 0.8 mm). The desired catalyst particle sizes were obtained by grinding and sieving a batch of calcined catalyst.

Figure 5.3.1 shows the conversion as function of time on stream for different catalyst particle sizes. Only the smallest catalyst fraction behaves differently : it deactivates more

strongly. This can be explained by the fact that the smallest particle size has the highest specific surface area (m^2/m^3) from which lithium components can volatilize more easily due to the shortest path for lithium salts to diffuse to the outer surface.

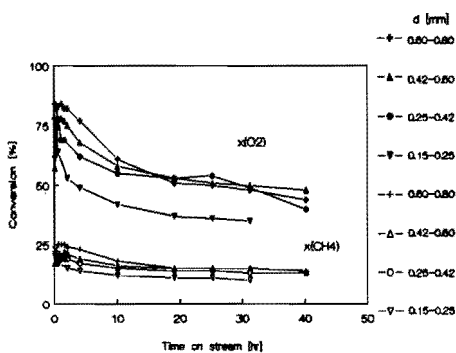


Figure 5.3.1. Methane ($x\text{CH}_4$) and oxygen ($x\text{O}_2$) conversion as function of time on stream for different particle sizes. $T=800^\circ\text{C}$, $\text{CH}_4/\text{O}_2=5$, $W/F=0.3$ g.s/ml.

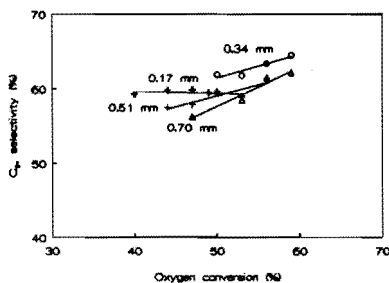


Figure 5.3.2. Product selectivity versus oxygen conversion for different particle sizes. $T=800^\circ\text{C}$, $\text{CH}_4/\text{O}_2=5$, $W/F=0.3$ g.s/ml.

Effects on the product selectivity are not present as shown in Figure 5.3.2, where the product selectivity is plotted against the oxygen conversion. This is confirmed by transport limitation calculations when applying suitable criteria². Follmer et al.³ investigated the influence of particle sizes of 0.1 mm to 4 mm on methane coupling at 1013K over Na/CaO and found that the smallest particle sizes show no diffusion limitations in agreement with our measurements.

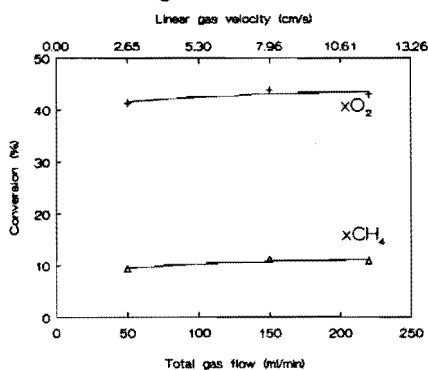


Figure 5.3.3. Methane ($x\text{CH}_4$) and oxygen ($x\text{O}_2$) conversion as function of the flow-rate. $T=800^\circ\text{C}$, $\text{CH}_4/\text{O}_2=5$, $W/F=0.3$ g.s/ml.

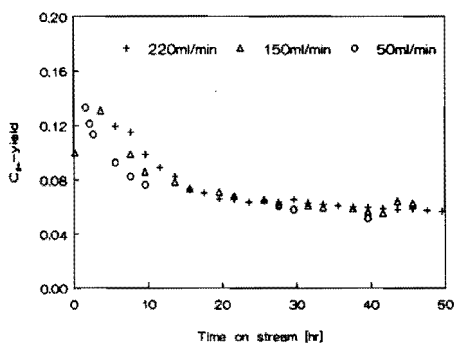


Figure 5.3.4. C_{2+} yield as function of the runtime for different flow-rates. $T=800^\circ\text{C}$, $\text{CH}_4/\text{O}_2=5$, $W/F=0.3$ g.s/ml.

For the large particle sizes ($> 1\text{mm}$) Follmer et al. reported a beneficial effect of pore diffusion limitations on the C_{2+} selectivity during methane coupling. The C_{2+} selectivity increased with the particle size. We did not test these large particle sizes as it is difficult to reach ideal plug-flow and isothermal temperature control with these large particle sizes in a laboratory reactor.

External diffusion limitations were tested by varying the linear gas velocity at constant contact time (W/F). Figure 5.3.3 shows the conversion as function of the total gas flow at constant W/F . It clearly shows that there is no effect of flow on the activity of the catalyst, at least at the linear gas velocities used here. Effect of the linear gas velocity on the C_{2+} yield, as shown in Figure 5.3.4., is also not present.

5.4 KINETIC MODELLING

This paragraph describes the results of differential kinetic measurements carried out in a micro fixed bed reactor as described previously. The aim is to model the catalytic methane coupling process according to the consecutive reaction mechanism proposed in Chapter 4 (paragraph 4.4).

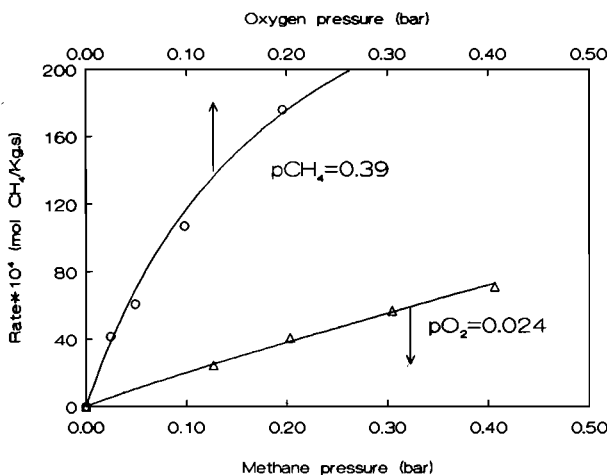


Figure 5.4.1. Methane disappearance rate during methane coupling over Li/MgO versus methane and oxygen pressure. $T=800^{\circ}\text{C}$, $W/F=0.03\text{ g.s/ml}$.

Figure 5.4.1 shows the reaction rate (r_m) as function of methane and oxygen partial pressure respectively. Correlating this result with the simple power rate equation leads to:

$$r_m = k_m * [P_{CH_4}]^a * [P_{O_2}]^b$$

$$a = 0.91 \pm 0.12$$

$$b = 0.62 \pm 0.13$$

$$k_m = 0.145 \pm 0.015 \text{ mole CH}_4/(\text{kg cat.}(\text{bar})^{a+b}.\text{s})$$

with pressures in bar.

One can conclude from these data that the overall reaction rate is first order in methane and half order in oxygen. The order 0.5 with respect to oxygen can be explained in two ways: 1) Oxygen is rapidly and reversibly dissociated into "active surface atoms". The adsorption is weak, hence the concentration of surface oxygen atoms is proportional to the square root of the oxygen pressure. As a result the power law is correctly describing the kinetics. 2) Molecular oxygen is involved in the rate determining process. It is relatively strongly adsorbed. This may result in an apparent reaction order of 0.5, although an Eley - Rideal equation should fit the data better. Indeed it appears possible to fit our data to the following equation:

$$r_m = k_1 * [P_{CH_4}] * [P_{O_2}]/(1 + b_{O_2} * [P_{O_2}])$$

$$k_1 = 0.45 \text{ mole CH}_4/(\text{kg cat.}(\text{bar})^2.\text{s})$$

$$b_{O_2} = 5 (\text{bar})^{-1}$$

with pressures in bar.

This is in agreement with the results from the transient experiments (Chapter 3). Based on this mechanism of methane activation the consecutive reaction mechanism was described according to the following rate equations:

$$r_i = k_i * p_i * p_{O_2}/(1 + b_{O_2} * p_{O_2})$$

Thus the hydrocarbon molecules CH_4 , C_2H_6 or C_2H_4 and CO are assumed to react from the gas phase with an adsorbed oxygen species. The contribution of parallel reactions in the gas phase is accounted for by adjusting the k-values. It is therefore assumed that radical initiation reactions mainly take place at the catalyst surface. Consecutive reactions in the gas phase, leading to the next stable molecule in the series are considered infinitely fast. Thus the net production rates (R_i) of each of the components follow from the material balances:

$$R_{CH_4} = -r_{CH_4}$$

$$R_{C_2H_6} = 0.5r_{CH_4} - r_{C_2H_6}$$

$$R_{C_2H_4} = r_{C_2H_6} - r_{C_2H_4}$$

$$R_{CO} = 2r_{C_2H_4} - r_{CO}$$

$$R_{CO_2} = r_{CO}$$

Using the appropriate stoichiometry factors, R_{O_2} is easily formulated to complete the above equations.

The k -values were determined by fitting the model to the results of integral kinetic measurements collected in our laboratory. A non-linear least squares estimation routine based on Marquardt's method⁴ was applied. The parameter b_{O_2} was fixed at a value of 5 (bar)^{-1} , as determined previously. Furthermore a distinction was made between data obtained with a fresh catalyst samples and data from experiments with an aged catalyst. The results with respect to the k -values are presented in Table 5.4.1.

Table 5.4.1. k -Values (mole/kg cat.s.(bar)²) resulting from parameter fitting of integral methane coupling experiments over Li/MgO. $T=800^\circ\text{C}$, $CH_4/O_2=5$, $p_{He}=0.4 \text{ bar}$, $b_{O_2}=5 \text{ (bar)}^{-1}$

| Catalyst | k_{CH_4} | $k_{C_2H_6}$ | $k_{C_2H_4}$ | k_{CO} | $k_{C_2H_4}/k_{CH_4}$ |
|----------|------------|--------------|--------------|----------|-----------------------|
| Aged | 0.65 | 37 | 12 | 1.6 | 19 |
| Fresh | 2.4 | 47 | 16 | 100 | 6.3 |

The case of the aged catalyst is interesting as a reference, because one can assume that the catalyst is playing a minor role here. This is confirmed by the comparison of selectivity data of the aged catalyst with results of an empty reactor, both as a function of the oxygen conversion (Figure 5.4.2). The results are indeed very similar, indicating that homogeneous reactions (gas phase) predominate during the experiments with the aged catalyst. A reasonable fit of measured and calculated selectivities has been obtained both for the fresh as for the aged catalyst. Figure 5.4.3. shows the product selectivity versus W/F for the case of the aged catalyst (symbols) and the calculated selectivities (lines). As can be seen a reasonable fit has been achieved with the highest accuracy at the largest contact times and the poorest accuracy at the smallest contact times. This is not surprising as the experimental error is the largest at the smallest W/F . Also the fact has to be considered that the model is no longer appropriate at very low conversion levels, because at very small contact times the direct oxidation of methane to carbon dioxide can no longer be neglected. For the case of the fresh catalyst it is very difficult to obtain an accurate selectivity pattern as function of the contact time, due to the fast deactivation of the Li/MgO catalyst. Therefore no accurate selectivity fit versus W/F could be performed. On the other hand it is possible to fit the results of the optimal selectivities obtained at a certain W/F (0.3 g.s/ml). This is shown in Table 5.4.2. By only changing the $k_{C_2H_4}/k_{CH_4}$ and the k_{CO} value the measured selectivities of a methane oxidation experiment over a fresh Li/MgO catalyst can be fitted quite well.

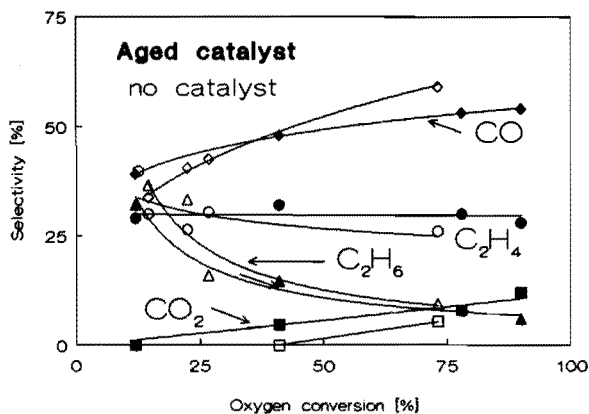


Figure 5.4.2. Product selectivity versus oxygen conversion for an aged Li/MgO catalyst and gas phase methane coupling. $T=800^{\circ}\text{C}$, $\text{CH}_4/\text{O}_2=5$.

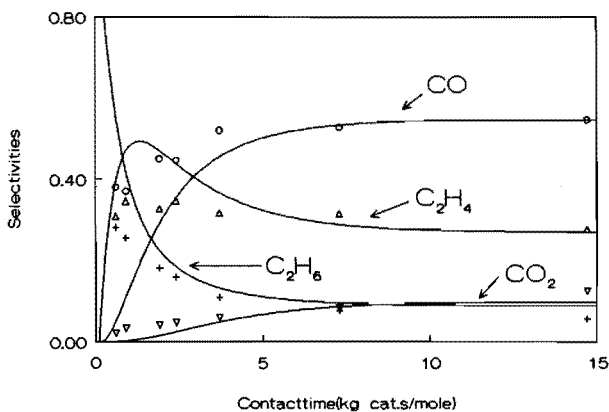


Figure 5.4.3. Product selectivity versus contact time (W/F) for experiment (symbols) and consecutive model fit. $T=800^{\circ}\text{C}$, $P=1\text{ bar}$, $\text{CH}_4/\text{O}_2=5$, Li/MgO catalyst.

Regarding the calculated k -values in Table 5.4.1., some interesting conclusion can be drawn, in connection with the low pressure results of Table 4.4.1. (Chapter 4). The ratio of $k_{\text{C}_2\text{H}_4}/k_{\text{CH}_4}$ is much higher for the atmospheric experiments than for the low pressure experiments (atmospheric (fresh catalyst) 6.3; low pressure 2.6). This increase in $k_{\text{C}_2\text{H}_4}/k_{\text{CH}_4}$ ratio can be ascribed to the contribution of gas phase reactions to the oxidation of ethylene at atmospheric pressure. The importance of the gas phase reactions is confirmed by the data of the aged catalyst: ageing of the catalyst has much more effect on k_{CH_4} and k_{CO} ("catalytic steps") than on $k_{\text{C}_2\text{H}_6}$ and $k_{\text{C}_2\text{H}_4}$.

Table 5.4.2. Comparison between experimental (fresh catalyst) and consecutive model fitting results. k -Values used from table 5.4.1.

| Selectivity (%) | Experiment | Fit |
|------------------|------------|------|
| C_2H_6 | 20 | 20 |
| C_2H_4 | 45 | 45 |
| CO | 7 | 6.7 |
| CO_2 | 28 | 28.3 |
| CH_4 conv. (%) | 23 | 21 |
| O_2 conv. (%) | 90 | 100 |

Table 5.4.3. C_{2+} yield as function of the $k_{C_2H_4}/k_{CH_4}$ ratio for the consecutive model. $CH_4/O_2=5$, $pHe=0.4$ bar.

| $k_{C_2H_4}/k_{CH_4}$ | C_{2+} Yield |
|-----------------------|----------------|
| 2.6 | 35 |
| 6.3 | 14 |
| 19 | 6 |

The $k_{C_2H_4}/k_{CH_4}$ ratio is the key factor in the selectivity of the methane oxidative coupling process, as demonstrated in Table 5.4.3, where the maximum yields are calculated for the three cases that correspond to the theoretical case (low pressure data), the fresh catalyst, and the aged catalyst. A catalyst influences the $k_{C_2H_4}/k_{CH_4}$ ratio by increasing the methane activation rate more than the ethylene activation rate. The ethylene activation rate is mainly determined by the gas phase activation rate. Therefore the high C_{2+} yields obtained by a catalyst are mainly due to the increase of the methane activation rate relative to the ethylene activation rate. The function of the catalyst may thus be reduced to a radical initiator, which releases radicals into the gas phase, without further interfering with the course of the reaction. The catalyst releases (methyl) radicals into the gas phase at a much higher rate than that the radicals are produced in the gas phase. In this way the catalyst increases the methyl radical concentration and may cause relatively high reaction rates to ethane, as the coupling is second order in methyl radicals, while the oxidation is probably first order. This reasoning is visualized by the simplified reaction scheme in Figure 5.4.4. Reaction 1 is the abstraction of a hydrogen atom from methane. Reaction 2 is the coupling reaction of the methyl radicals to C_{2+} components. Reaction 3 and 4 are the total oxidation reactions in which C-O bonds are formed irreversibly. In this way the catalyst favours the consecutive model.

The role of the catalyst as a methyl radical producer is supported by calculations with a computer model that simulates the gas phase methane oxidation by taking account of practically all elementary radical reactions.⁵ The effect of the catalyst is simulated by adding a set of reactions, which equals the overall reaction: $4CH_4 + O_2 \rightarrow 4CH_3 + 2H_2O$. The rate of formation of methyl radicals is increased, without increasing the C_{2+} oxidation reactions. The results of the computer simulations are shown in Table 5.4.4⁶. This Table shows a comparison between two simulations: with and without increased

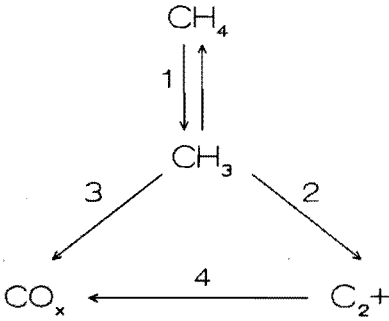


Figure 5.4.4. Simplified reaction scheme for the oxidative coupling of methane.

methyl radical production. At the same contact time, the higher methyl radical production rate increases both the methane and oxygen conversion, as expected, while the C_{2+} selectivity is somewhat lower. However, when results at the same conversion level are compared (first and last column of Table 5.4.4) it is clear that much higher selectivities are achieved at increased methyl radical production rate, in accordance with the hypothesis proposed.

Table 5.4.4. Computer simulations of gas phase oxidative coupling of methane with increased methyl radical production⁶.

| Methyl radical production | | Normal | Increased | |
|-----------------------------|-----|--------|-----------|------|
| Contact time | (s) | 2.7 | 2.7 | 0.13 |
| CH ₄ conversion | (%) | 0.06 | 3.4 | 0.09 |
| O ₂ conversion | (%) | 0.1 | 8.2 | 0.1 |
| C ₂₊ selectivity | (%) | 79 | 70 | 97 |
| CO _x selectivity | (%) | 21 | 30 | 3 |

Thus a selective coupling catalyst has to be a very active one, in order to arrive at a favourable low $k_{C_2H_4}/k_{CH_4}$ ratio, the key factor for the C_{2+} selectivity.

5.5 CONCLUSIONS

Catalyst deactivation is a continuous process, which limits the time scale on which the kinetic measurements should be performed.

There are no transport limitations at the reaction conditions applied ($T=800^\circ\text{C}$, $W/F=0.3 \text{ g.s/ml}$).

The overall kinetics of the oxidative coupling of methane over Li/MgO catalyst were determined by differential measurements. The results can be summarized:

$$r_{CH_4} = 0.145 \pm 0.015 \cdot P_{CH_4}^{0.91-0.12} \cdot P_{O_2}^{0.62-0.13} \text{ mole CH}_4/\text{kg. s.}$$

with pressures in bar.

The kinetics can be well described with an ELEY-RIDEAL kind of mechanism in which methane from the gas phase reacts with an adsorbed oxygen species on the catalyst surface.

The product selectivity can be modelled quite well with an assumed consecutive reaction model. From the modelling results it is clear that the reaction mechanism of the methane coupling process consists of heterogeneous and homogeneous reaction steps. The $k_{\text{C}_2\text{H}_4}/k_{\text{CH}_4}$ ratio is the key factor, which determines the product selectivity. A catalyst decreases the $k_{\text{C}_2\text{H}_4}/k_{\text{CH}_4}$ ratio by speeding up the methane activation rate relative to the ethylene activation rate. A fresh Li/MgO catalyst is capable of C_2+ yields of 15 - 19% ($k_{\text{C}_2\text{H}_4}/k_{\text{CH}_4} = 6.3$). Theoretically, however it seems possible to reach values over 25%. Further optimization of the interaction of homogeneous and heterogeneous reactions should make these yields achievable.

REFERENCES

1. S.J. Korf, PhD Thesis, University of Twente, Enschede, The Netherlands, 1990.
2. C.N. Satterfield, "Mass Transfer in Heterogeneous Catalysis", MIT Press, Cambridge, Mass., 1970.
3. G. Follmer, L. Lehmann and M. Baerns, *Catal. Today*, 4, 323 - 332 (1989).
4. D.W. Marquardt, *J. Soc. Indust. Appl. Math.*, 11 (2), 431 -441 (1963).
5. J.W.M.H. Geerts, Q. Chen, J.M.N. van Kasteren and K. van der Wiele, *Catal. Today*, 6, 519 - 526 (1990).
6. J.M.N. van Kasteren, J.W.M.H. Geerts and K. van der Wiele, *Stud. Surf. Sci. Catal.*, 55, 343 - 352 (1990).

CHAPTER 6

FINAL DISCUSSION

Lithium doped MgO used as catalyst for the oxidative coupling of methane has been investigated extensively in this work. The activity of the Li/MgO catalyst for methane activation is due to the presence of lithium. Very small amounts of lithium are sufficient to create an active and selective coupling catalyst. Lithium carbonate is a liquid at reaction temperatures of 720°C and higher. This explains the mobility of the lithium phase at the reaction temperatures. Deactivation of the Li/MgO catalyst is caused by lithium loss. The lithium loss is mainly due to evaporation of LiOH, which is formed during the course of the reaction by the reaction of water with the lithium carbonate in the catalyst.

Steady-state isotopic transient kinetic analysis (SSITKA) experiments with $\text{CH}_4/^{18}\text{O}_2$ and $^{13}\text{CH}_4/\text{O}_2$ have revealed that there is a pool of active oxygen species adsorbed at the catalyst surface. These active oxygen species are capable of hydrogen abstraction from methane very effectively. There is no pool of carbon containing species at the catalyst surface, which is actually taking part in the catalytic cycle. Methane is not adsorbed at the catalyst surface, but reacts from the gas phase with the active oxygen species. Therefore, an Eley - Rideal mechanism in which methane reacts from the gas phase with an adsorbed oxygen species seems most suitable for the Li/MgO catalyst system. Kinetic measurements confirm the applicability of this model to the methane coupling process over Li/MgO. The exact nature of the active oxygen species on Li/MgO is not clear. It can be both a mono-atomic as well as a di-atomic species.

The product distribution is the result of a consecutive reaction mechanism involving both homogeneous as well as heterogeneous reaction steps:



Low pressure experiments have revealed the role of the homogeneous gas phase reactions. At the catalyst surface hydrogen abstraction from methane takes place and methyl radicals are released into the gas phase. There ethane is formed by coupling of the methyl radicals. A small part of the methyl radicals is directly oxidized at the catalyst surface to CO_2 (not shown in the reaction scheme). The ethane dehydrogenation and ethylene oxidation step take place both in the gas phase and on the catalyst surface. The CO oxidation to CO_2 is definitely a catalytic reaction step.

From admixing experiments it was deduced that ethane and ethylene react at least a factor 2 faster than methane with Li/MgO. This limits the C_{2+} yield to a maximum. In the ideal (theoretical) case C_{2+} yields of 35% should be possible with Li/MgO. However, modelling of realistic measurements shows that the activation of ethylene is

mainly due to gas phase reactions. A catalyst strongly influences the ethylene to methane activation rate by increasing the methane activation rate more than the ethylene activation rate, thus lowering the $k_{C_2H_4}/k_{CH_4}$ ratio and enabling high C_{2+} yields. The Li/MgO catalyst lowers the $k_{C_2H_4}/k_{CH_4}$ ratio to 6.3, improving the C_{2+} yield by a factor of 2.5 compared to homogeneous oxidative coupling of methane (pure gas phase). Further optimization of the interaction of heterogeneous and homogeneous reactions should bring C_{2+} yields of 25% within reach, which are needed for an economically attractive process¹.

Future investigations should focus on the determination of the optimum interaction of gas phase and catalytic reaction steps and on the reduction of the lithium loss during reaction conditions. As in the oxidative coupling of methane always water will be formed in large amounts LiOH can readily be formed. The evaporation of the LiOH causes lithium loss and thus results in deactivation of the catalyst. This puts serious restraints on the lifetime of the Li/MgO catalyst. The lithium loss can be lowered by lowering of the reaction temperature, which will slow down the rate of evaporation of LiOH. Disadvantage of a low reaction temperature is the loss in activity for the methane activation relative to the ethylene activation rate, thus lowering the C_{2+} yield.

In a way of solving this dilemma doping the Li/MgO catalyst with metal oxides like SnO_2 or CeO_2 seems a solution. Korf² has shown that with Li/Sn/MgO C_{2+} yields of 12% can be reached at 700°C. The lithium loss is lowered not only by applying a lower reaction temperature, but also by an interaction of Sn with the lithium. The added amount of Sn must be very low (0.029 mmol/g catalyst), because addition of high amounts of Sn results in an decrease of C_{2+} selectivity. That lithium interacts with impurities in the catalyst can be shown by Electron Paramagnetic Resonance (EPR) measurements.

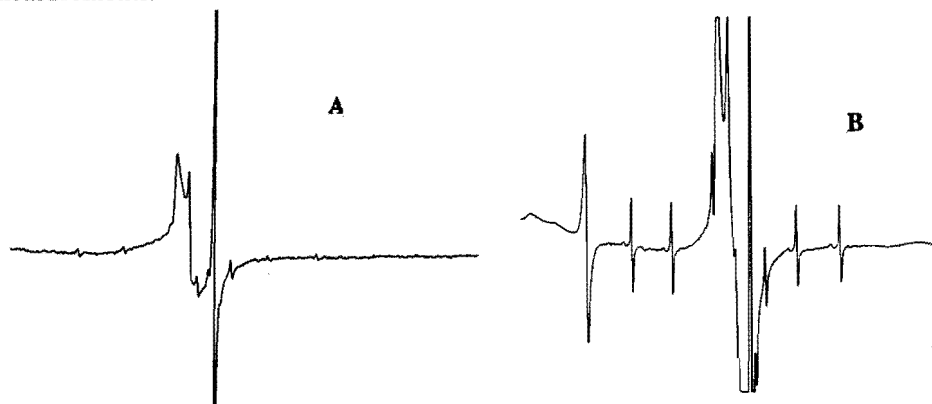


Figure 6.1. EPR spectra of pure (A) and Li doped MgO (B) at 100K.

Figure 6.1 depicts the EPR spectra of pure MgO and Li/MgO. The peaks are all due to paramagnetic impurities in the catalyst with Fe^{3+} , Cr^{3+} and Mn^{2+} as the main sources³. Addition of lithium to the MgO leads to stabilization of the Mn^{2+} in the MgO lattice. In pure MgO the Mn^{2+} peaks are hardly detectable while in Li/MgO the Mn^{2+} peaks are very intense. Lithium interacts with the Mn^{2+} impurity in the catalyst. Addition of small amounts of Sn oxide show no great effects on the EPR spectrum of Li/MgO. More interesting is the effect of Sn addition on the Li^+O^- centra which play an important role in the methane coupling process according to Driscoll et al⁴. Figure 6.2 shows the EPR spectra of Li/MgO and Li/Sn/MgO heated to 800°C in air and rapidly quenched in liquid nitrogen. At $g=2.054$ the Li^+O^- peak can be seen in Li/MgO while in Li/Sn/MgO the same peak is changed. Clearly this indicates the occurrence of an interaction between Sn and lithium present in the MgO lattice. This interaction probably explains the lower lithium loss of this doped Li/MgO catalyst. The higher activity of this catalyst compared to undoped Li/MgO is due to the addition of extra active centres (SnO_2).

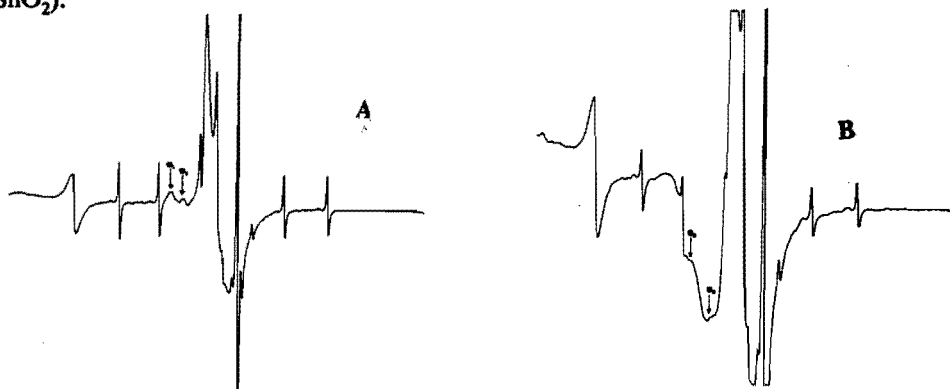


Figure 6.2. EPR spectra of Li doped MgO (A) and Li/Sn/MgO (B) quenched in liquid nitrogen after heating in air at 800°C.

At large additions of SnO_2 the SnO_2 will predominate the catalyst. This does not result in an improvement of the $k_{\text{C}_2\text{H}_4}/k_{\text{CH}_4}$ ratio or an improvement of the C_{2+} yield.

Summarizing it can be stated that Li/MgO catalyst modifications are needed to prevent its rapid deactivation, which is the main disadvantage of this catalytic system. Further optimization of the interaction between gas phase and catalytic reactions should make high C_{2+} yields possible. These modifications and optimizations are necessary to get a catalytic system, which can be used for an economical feasible oxidative coupling process.

REFERENCES

1. J.W.M.H. Geerts, PhD Thesis, Eindhoven, The Netherlands, (1990).
2. S.J. Korf, PhD Thesis, University of Twente, Enschede, The Netherlands (1990).
3. Y. Chen, H.T. Tohver, J. Narayan and M.M. Abraham, *Phys. Rev. B*, 16 (12), 5535-5542 (1977).
4. D.J. Driscoll, W. Martir, J-X Wang and J.H. Lunsford, *J. Am. Chem. Soc.*, 107, 58-63 (1985).

LIST OF PUBLICATIONS

1. J.M.N. van Kasteren, J.W.M.H. Geerts and K. van der Wiele, Ethylene synthesis by catalytic oxidation of methane over Li-doped MgO catalysts: The interaction of catalytic and non-catalytic reaction steps, Proc. 9th I.C.C. , Eds. M.J. Phillips and M. Ternan, Calgary, Alberta, Canada, 2, 1988, 930-936.
2. J.W.M.H. Geerts, J.M.N. van Kasteren and K. van der Wiele, A mechanistic study on the oxidative coupling of methane over lithium doped magnesium oxide catalysts, Proc. EC. Congress: "Hydrocarbons: Source of energy", Eds. G. Imarisio, M. Frias and J.M. Bemtgen, Lyon, France, 1988, 434-440.
3. J.W.M.H. Geerts, J.M.N. van Kasteren and K. van der Wiele, The investigation of individual reaction steps in the oxidative coupling of methane over lithium doped magnesium oxide, Catal. Today, 4, 1989, 453-461.
4. J.M.N. van Kasteren, J.W.M.H. Geerts and K. van der Wiele, The role of heterogeneous reaction steps during the oxidative coupling of methane over Li/MgO catalysts, Catal. Today, 6, 1990, 497-502.
5. J.W.M.H. Geerts, Q. Chen, J.M.N. van Kasteren and K. van der Wiele, Thermodynamics and kinetic modelling of the homogeneous gas phase reactions of the oxidative coupling of methane, Catal. Today., 6, 1990, 519-526.
6. J.M.N. van Kasteren, J.W.M.H. Geerts and K. van der Wiele, Working principle of Li doped MgO applied for the oxidative coupling of methane, Preprints first World Congress: "New developments in selective oxidation", Rimini, Italy, september 18 - 22, 1989; Stud. Surf. Sci. Catal., 55, 1990, 343-349.
7. J.W.M.H. Geerts, J.M.N. van Kasteren and K. van der Wiele, Molten salts as catalysts for the oxidative coupling of methane, J. Chem. Soc., Chem. Commun., 1990, 802-803.

8. J.W.M.H. Geerts, J.M.N. van Kasteren and K. van der Wiele, Ethylene from natural gas by direct catalytic oxidation, EC contract EN3C-0038-NL (GDF), Final Report, 1990.
9. J.W.M.H. Geerts, J.M.N. van Kasteren and K. van der Wiele, Ethylene from natural gas by direct catalytic oxidation, EC contract EN3C-0038-NL (GDF), Summary Report, 1990.
10. J.R.H. Ross, J.A. Roos en S.J. Korf, K. van der Wiele, J.W.M.H. Geerts en J.M.N. van Kasteren, Etheen uit aardgas door katalytische oxidatieve koppeling van methaan met behulp van zuurstof, SON Jaarverslag 1987, 101-106.
11. J.M.N. van Kasteren, P. de Been and J.G.A. Hölscher, The formation of higher hydrocarbons from methane in a column discharge in hydrogen or argon, 9th Eur. Sect. Conf. on atomic and molecular physics of ionized gases, Escampig 88, Lissbon, 1988, 351-352.
12. J.M.N. van Kasteren, J.W.M.H. Geerts and K. van der Wiele, Methane oxidative coupling using Li/MgO catalysts: The importance of consecutive reactions, Presented at: 9th International Symposium on C₁-reactions, Oslo, Norway, August 13 - 17, 1990.
13. K. van der Wiele, J.W.M.H. Geerts and J.M.N. van Kasteren, Elementary reactions and kinetic modelling of the oxidative coupling of methane, To be published.

DANKWOORD

Voor het tot stand komen van dit proefschrift ben ik veel dank verschuldigd aan mijn eerste promotor prof. dr. ir. Kees van der Wiele voor zijn begeleiding, de vele gevoerde discussies en het vele, door hem verrichte correctiewerk. Daarnaast dank ik prof. dr. ir. G.B.M.M. Marin en dr. ir. J.H.B.J. Hoebink voor de nuttige discussies en adviezen tijdens mijn promotie onderzoek en de voltooiing van mijn proefschrift.

Een bijzonder woord van dank gaat uit naar mede promovendus Jan Geerts voor de prettige samenwerking tijdens dit promotie-onderzoek.

Verder ben ik dank verschuldigd aan de vaste staf onderzoeksmederkers: Ton Sommen, Paul Weymans, Bert Verhaar en Wim Groenland vooral voor hun ondersteunende activiteiten op praktisch, computer technisch en administratief nivo.

De in dit proefschrift beschreven experimenten zijn grotendeels tot stand gekomen dankzij het werk van vele afstudeerders en praktikanten. In het kader van hun ir. opleiding zijn met name bij dit promotiewerk betrokken geweest: Bert Bosman, Abu Saëbu, Piet Waalen, Guus van de Beek, Huub van Lier, Peter de Been, Philippe van der Meulen, Pieter Couwenberg en Frans van de Laar waarvoor mijn hartelijke dank. In het kader van het P-3 praktikum ben ik dank verschuldigd aan: R. Krishnasing, W. van Aerle, J. Sienkiewicz en R. Tacken die EPR metingen hebben uitgevoerd; R. Vossen, T. Dijkstra, P. Romer, R. Uitdewillegen, M. Eijssen, J. Altena, R. Dobbelaar, A. Rustidge, L. Sagis, A. van Neerven voor het katalysator ontwikkelwerk; P. Alers en M. van Eck voor de opbouw van de plasma reaktor.

Naast deze studenten mag de bijdrage van stagiaires niet vergeten worden: Roger van Hoek, Henk-Jan de Vos, Rob Josiassen en Marylene Timmermans die de katalysator desaktiveringsmetingen hebben uitgevoerd; Rob Richter, Jan Vermeir, Frank Janssen, Rob Dingemans en Ton Richters die automatiseringswerkzaamheden hebben verricht. Voor hun wezenlijke bijdragen ben ik hen zeer erkentelijk.

Binnen de TUE ben ik verder dank verschuldigd aan de technische staf van de Faculteit Scheikunde, met name Dirk Verschie, M. van der Heide en D. Francois en de glasblazerij en de elektronische werkplaats van de centrale technische dienst.

Bijzondere vermelding verdient de vakgroep Vaste Stof der faculteit Technische Natuurkunde, met name dr. ir. Hans Hölscher, voor de plezierige samenwerking in het kader van de plasmametingen.

Buiten de TUE ben ik dank verschuldigd aan het samenwerkingsverband met de Technische Universiteit Twente, de groep van prof. dr. J.R.H. Ross, met name Jan van Ommen, Stefan Korf en Jan Roos, en de samenwerking met prof. dr. B.K. Hodnett van het National Instituut for Higher Education (NIHE) te Limerick, Ierland. Bijzondere vermelding verdient prof. dr. ir. J.M.L. Penninger van AKZO, Hengelo, voor zijn bijdrage tot de vele discussies over het methaankoppelingsproces en de groep van prof.

dr. M. Baerns van de Ruhr-Universität te Bochum, West - Duitsland, voor de blikverruimende bijeenkomsten op het gebied van de methaankoppeling.

Tenslotte ben ik dank verschuldigd aan de Nederlandse Organisatie voor Wetenschappelijk Onderzoek (NWO), de Europese Gemeenschap (EG) en AKZO voor hun financiële ondersteuning van dit onderzoek.

LEVENSLLOOP

Johannes (HAN) Maria Nicolaas van Kasteren werd geboren op 3 november 1961 te Heerlen. Na de lagere school volgde hij het gymnasium aan het Bernardinus College te Heerlen. Na zijn eindexamen in 1980 begon hij in september 1980 aan de Technische Universiteit Eindhoven de studie Scheikundige Technologie welke in april 1986 afgerond werd door middel van een afstudeeronderzoek bij prof. ir. M. Tels op het gebied van de "Natte oxydatie" getiteld: "Corrosie onderzoek bij natte oxidatie van toxische componenten bij hoge temperatuur en druk". In mei 1986 begon hij als promovendus bij de vakgroep Chemische Proceskunde bij prof. dr. ir. K. van der Wiele met een onderzoek naar de directe katalytische omzetting van methaan in etheen. Werk dat uiteindelijk resulteerde in dit proefschrift.

Sinds mei 1990 vervult hij zijn vervangende dienstplicht bij het Interuniversitair Milieu-instituut Brabant (IMB).

STELLINGEN
behorende bij het proefschrift

OXIDATIVE COUPLING OF METHANE OVER LITHIUM PROMOTED MAGNESIA

van

Johannes Maria Nicolaas van Kasteren

- 1 De wisselwerking tussen katalytische en niet - katalytische reactiestappen is essentieel voor de produktie van hogere koolwaterstoffen door oxydatieve koppeling van methaan.
Hoofdstuk 4 van dit proefschrift.
J.M.N. van Kasteren, J.W.M.H. Geerts and K. van der Wiele, *Catal. Today*, 6, 447 - 502 (1990).
- 2 Het optreden van niet - katalytische reacties tijdens de oxydatieve koppeling van methaan heeft consequenties voor het reactorontwerp.
J.M.N. van Kasteren, J.W.M.H. Geerts and K. van der Wiele, *Proceedings 9th Int. Congr. on Catal.*, Eds. M.J. Phillips and M. Ternan, Calgary, Canada, 2, 930 - 936 (1988).
- 3 Yates en Zlotin verwaarlozen ten onrechte het effect van de prekatalytische ruimte bij de vergelijking tussen een lege en een met katalysator gevulde reactor.
D.J.C. Yates and N.F. Zlotin, *J. Cat.*, 11, 317 - 324 (1988).
- 4 In de correlatie tussen het lithiumgehalte van de Li/MgO katalysator en de activiteit gaan Baronetti e. a. voorbij aan het desaktiveringsgedrag van de Li/MgO katalysator. Het lithiumgehalte is een functie van de procesomstandigheden.
G.T. Baronetti, E.J. Lazzari, A.A. Castro and O.A. Scelza, *Stud. Surf. Sci. Catal.*, 55, 373 - 380 (1990).
- 5 De conclusie van Bartsch e. a. dat de regeneratie van de Li/MgO katalysatoren de snelheidsbepalende stap is in de oxydatieve koppeling van methaan, is onjuist.
S. Bartsch, J. Falkowski and H. Hofmann, *Catal. Today*, 4, 421 - 431 (1989).
S. Bartsch, H. Hofmann, *Stud. Surf. Sci. Catal.*, 55, 353 - 361 (1990).

6. De bewering van Miro e. a. dat een grote zuurstofopnamecapaciteit van het katalysatorrooster en een grote mobiliteit van de zuurstof daarin doorslaggevend zijn voor het bereiken van een hoge C_{2+} yield, is onjuist.
E.E. Miro, Z. Kalenik, J. Santamaria and E.E. Wolf, *Catal. Today*, 6, 511 - 518 (1990).
7. Martin e. a. suggereren ten onrechte dat de ethaan dehydrogenering tijdens de oxydatieve koppeling van methaan katalytisch van aard is.
G.A. Martin, P. Turlier, V. Ducarme, C. Mirodatos and M. Pinabiau, *Catal. Today*, 6, 373 - 380 (1990).
8. Bij de kinetische beschrijving van de methaanomzetting in een stille elektrische ontlading verwaarlozen Rutkowsky e. a. ten onrechte dat de vorming van ethaan hoofdzakelijk via de koppeling van twee methylradikalen plaatsvindt.
J. Rutkowsky, H. Drost and R. Mach, *Beitr. Plasmaphys.* 23 (2), 181 - 191 (1983).
9. In het streven naar een betere milieuzorg is het erkennen van het nut van "zachte" (niet - technische) wetenschap voor "harde" (technische) wetenschappers een harde dobber.
10. De voortgang in een bepaald onderzoeksgebied is omgekeerd evenredig met het aantal publikaties in dat gebied.

Eindhoven, november 1990.